Table 1 criteria was significantly lower in V1–V14 (12.0 ± 5.0), than in N1–N57 (20.9 ± 4.0, $p < 0.0001$). These data suggested that our criteria do not simply reflect the presence of hepatitis virus infection, inflammation or fibrosis at the chronic hepatitis and liver cirrhosis stages, but in fact reflect the carcinogenetic risk itself.

Discussion

For appropriate surveillance of patients at the precancerous stage for HCCs, the criteria for carcinogenetic risk estimation should be explored. As considerable numbers of liver tissue samples obtained from patients with HBV or HCV infection indicate a future risk of HCCs, even if HCCs are not yet present, comparison between liver tissue samples obtained from patients with HBV or HCV infection but without HCCs and those obtained from patients with HBV or HCV infection but also showing HCCs, is not an adequate strategy for establishing criteria for carcinogenetic risk estimation. Therefore, in our previous study, we focused on BAC clones whose signal ratios differed significantly between samples of normal liver tissue obtained from patients without HBV or HCV infection and samples of noncancerous liver tissue obtained from patients with HCCs (namely BAC clones on which DNA methylation alterations had occurred at the precancerous stage), and also those on which such DNA methylation alterations had been inherited by HCCs themselves from precancerous conditions. In this way, we successfully established such criteria using BAC array-based methods.[18]

In our study, the reliability of BAMCA was again confirmed: BAMCA was able to provide an overview of DNA methylation tendency in large regions of chromosomes, and especially was able to detect DNA methylation alterations occurring in a coordinated manner in the entire BAC region. However, the exact CpG sites that are of diagnostic impact are unclear, because several *Xma* I/*Sma* I sites that are effective in BAMCA generally exist on each of the BAC clones with an average insert size of 170 kbp.[20] Moreover, as BAMCA requires a large amount of genomic DNA, and the technique is somewhat cumbersome, our previous criteria based on BAMCA may not be suitable for clinical uses such as risk estimation based on liver biopsy specimens. Therefore, we employed Pyrosequencing™ technology, which is an excellent tool for quantitative estimation of DNA methylation levels at specific CpG sites.

Although numerous *Xma* I/*Sma* I sites are located within CpG islands, one or two *Xma* I/*Sma* I sites on each CpG island were analyzed because of difficulties with the design of the PCR and sequencing primers. Then, DNA methylation levels at 203 CpG sites on the 25 BAC clones that comprised our previous criteria based on BAMCA were evaluated quantitatively by pyrosequencing. By combining the 30 regions including 45 specific CpG sites, which were revealed to have a large diagnostic impact, the specificity of the criteria for carcinogenetic risk estimation was successfully improved in comparison with our previous criteria based on BAMCA[18]: the sensitivity and specificity of the criteria after revision by pyrosequencing were both 100% in the learning cohort and were 95.6% and 100% in the validation cohort, respectively.

Only one region (region 20 in Table 1) among 30 regions that had been used for defining the revised criteria for carcinogenetic risk estimation was located within the promoter region of a specific gene (general receptor for phosphoinositides 1-associated scaffold protein), although DNA methylation alterations in promoter regions are known to be one of most consistent epigenetic changes in human cancers.[24] At the risk stage, but not in established cancers, it is feasible that DNA methylation alterations do not expand immediately to the promoter regions of specific genes, such as tumor-related genes. However, 20, 19 and 9 regions that had been used for defining the revised criteria were located within gene bodies, non-CpG islands, and noncoding regions, respectively, which have been overlooked as targets of DNA methylation alterations during multistage human carcinogenesis. Although most of the recently developed detection technologies, such as promoter arrays and CpG island arrays, are sequence-based methods and cannot comprehensively measure the DNA methylation status of gene bodies, non-CpG islands and noncoding regions,[25,26] our findings indicate that meticulous examination of such sequences is also important for establishment of optimal diagnostic indicators.

DNA methylation status in the 30 regions in noncancerous liver tissue at the precancerous stage was significantly correlated with both cancer-free and overall survival rates of patients with HCCs (Fig. 4). Although prognostication before development of HCCs was not a clinically relevant issue, and we never intended to perform such prognostication, we can consider that DNA methylation alterations determining patient outcome had already accumulated at the precancerous stage, based on the data in Figure 4. As DNA methylation status is not randomly altered at the precancerous stage, and DNA methylation profiles in noncancerous liver tissue have been proven to be clinicopathologically valid, it is feasible that such profiles could be optimal indicators for carcinogenetic risk estimation.

The difference in the number of regions satisfying the criteria listed in Table 1 between liver tissue samples showing chronic hepatitis and those showing cirrhosis was marginal, indicating that our criteria were not simply associated with inflammation or fibrosis. In addition, the average number of regions satisfying the Table 1 criteria were significantly lower in liver tissue from patients without HCCs (V1–V14) than in noncancerous liver tissue from patients with HCCs (N1–N34), even though the patients from whom V1–V14 were obtained were infected with HBV or HCV. DNA methylation status in the 30 regions does not depend on hepatitis virus infection but may actually reflect the carcinogenetic risk itself. Therefore, our criteria not only discriminate noncancerous liver tissue from patients with HCCs from normal liver tissues but also may be applicable for classifying liver tissue obtained from patients who are being followed up

because of HBV or HCV infections, chronic hepatitis or cirrhosis into that which may generate HCCs and that which will not.

During surveillance at the precancerous stage, to reveal the baseline liver histology, microscopic examination of liver biopsy specimens is performed in patients with HBV or HCV infection before interferon therapy.[27,28] Therefore, carcinogenetic risk estimation using such liver biopsy specimens will be advantageous for close follow-up of patients who are at high risk of HCC development. We have confirmed that pyrosequencing can be performed using a very small amount of degraded DNA extracted from formalin-fixed and paraffin-embedded liver biopsy specimens (unpublished data). We now intend to prospectively validate the reliability of risk estimation based on the revised criteria using pyrosequencing in liver biopsy specimens obtained before interferon therapy from a large cohort of patients with HBV or HCV infection.

Acknowledgements

Author R.N. received a Research Resident Fellowship from the Foundation for Promotion of Cancer Research in Japan.

References

1. Chang MH, Chen CJ, Lai MS, Hsu HM, Wu TC, Kong MS, Liang DC, Shau WY, Chen DS. Universal hepatitis B vaccination in Taiwan and the incidence of hepatocellular carcinoma in children. Taiwan Childhood Hepatoma Study Group. *N Engl J Med* 1997;336:1855–9.
2. Tanaka Y, Hanada K, Mizokami M, Yeo AE, Shih JW, Gojobori T, Alter HJ. Inaugural article: a comparison of the molecular clock of hepatitis C virus in the United States and Japan predicts that hepatocellular carcinoma incidence in the United States will increase over the next two decades. *Proc Natl Acad Sci USA* 2002; 99:15584–9.
3. Jones PA, Baylin SB. The epigenomics of cancer. *Cell* 2007;128:683–92.
4. Sharma S, Kelly TK, Jones PA. Epigenetics in Cancer. *Carcinogenesis* 2009;31:27–36.
5. Kanai Y, Hirohashi S. Alterations of DNA methylation associated with abnormalities of DNA methyltransferases in human cancers during transition from a precancerous to a malignant state. *Carcinogenesis* 2007;28:2434–42.
6. Kanai Y. Alterations of DNA methylation and clinicopathological diversity of human cancers. *Pathol Int* 2008;58:544–58.
7. Kanai Y, Ushijima S, Tsuda H, Sakamoto M, Sugimura T, Hirohashi S. Aberrant DNA methylation on chromosome 16 is an early event in hepatocarcinogenesis. *Jpn J Cancer Res* 1996;87:1210–7.
8. Kondo Y, Kanai Y, Sakamoto M, Mizokami M, Ueda R, Hirohashi S. Genetic instability and aberrant DNA methylation in chronic hepatitis and cirrhosis—a comprehensive study of loss of heterozygosity and microsatellite instability at 39 loci and DNA hypermethylation on 8 CpG islands in microdissected specimens from patients with hepatocellular carcinoma. *Hepatology* 2000;32:970–9.
9. Kaneto H, Sasaki S, Yamamoto H, Itoh F, Toyota M, Suzuki H, Ozeki I, Iwata N, Ohmura T, Satoh T, Karino Y, Satoh T, et al. Detection of hypermethylation of the p16(INK4A) gene promoter in chronic hepatitis and cirrhosis associated with hepatitis B or C virus. *Gut* 2001; 48:372–7.
10. Saito Y, Kanai Y, Sakamoto M, Saito H, Ishii H, Hirohashi S. Overexpression of a splice variant of DNA methyltransferase 3b. DNMT3b4, associated with DNA hypomethylation on pericentromeric satellite regions during human hepatocarcinogenesis. *Proc Natl Acad Sci USA* 2002;99:10060–5.
11. Saito Y, Kanai Y, Nakagawa T, Sakamoto M, Saito H, Ishii H, Hirohashi S. Increased protein expression of DNA methyltransferase (DNMT) 1 is significantly correlated with the malignant potential and poor prognosis of human hepatocellular carcinomas. *Int J Cancer* 2003;105:527–32.
12. Kanai Y. Genome-wide DNA methylation profiles in precancerous conditions and cancers. *Cancer Sci* 2009;101:36–45.
13. Arai E, Kanai Y. DNA methylation profiles in precancerous tissue and cancers: carcinogenetic risk estimation and prognostication based on DNA methylation status. *Epigenomics* 2010;2: 467–81.
14. Misawa A, Inoue J, Sugino Y, Hosoi H, Sugimoto T, Hosoda F, Ohki M, Imoto I, Inazawa J. Methylation-associated silencing of the nuclear receptor 1I2 gene in advanced-type neuroblastomas, identified by bacterial artificial chromosome array-based methylated CpG island amplification. *Cancer Res* 2005;65:10233–42.
15. Sugino Y, Misawa A, Inoue J, Kitagawa M, Hosoi H, Sugimoto T, Imoto I, Inazawa J. Epigenetic silencing of prostaglandin E receptor 2 (PTGER2) is associated with progression of neuroblastomas. *Oncogene* 2007;26:7401–13.
16. Tanaka K, Imoto I, Inoue J, Kozaki K, Tsuda H, Shimada Y, Aiko S, Yoshizumi Y, Iwai T, Kawano T, Inazawa J. Frequent methylation-associated silencing of a candidate tumor-suppressor, CRABP1, in esophageal squamous-cell carcinoma. *Oncogene* 2007;26:6456–68.
17. Arai E, Ushijima S, Fujimoto H, Hosoda F, Shibata T, Kondo T, Yokoi S, Imoto I, Inazawa J, Hirohashi S, Kanai Y. Genome-wide DNA methylation profiles in both precancerous conditions and clear cell renal cell carcinomas are correlated with malignant potential and patient outcome. *Carcinogenesis* 2009;30:214–21.
18. Arai E, Ushijima S, Gotoh M, Ojima H, Kosuge T, Hosoda F, Shibata T, Kondo Y, Yokoi S, Imoto I, Inazawa J, Hirohashi S, et al. Genome-wide DNA methylation profiles in liver tissue at the precancerous stage and in hepatocellular carcinoma. *Int J Cancer* 2009;125:2854–62.
19. Nishiyama N, Arai E, Chihara Y, Fujimoto H, Hosoda F, Shibata T, Kondo T, Tsukamoto T, Yokoi S, Imoto I, Inazawa J, Hirohashi S, et al. Genome-wide DNA methylation profiles in urothelial carcinomas and urothelia at the precancerous stage. *Cancer Sci* 2010;101: 231–40.
20. Osoegawa K, Mammoser AG, Wu C, Frengen E, Zeng C, Catanese JJ, de Jong PJ. A bacterial artificial chromosome library for sequencing the complete human genome. *Genome Res* 2001;11: 483–96.
21. Clark SJ, Harrison J, Paul CL, Frommer M. High sensitivity mapping of methylated cytosines. *Nucleic Acids Res* 1994;22: 2990–7.
22. Shen L, Guo Y, Chen X, Ahmed S, Issa JP. Optimizing annealing temperature overcomes bias in bisulfite PCR methylation analysis. *Bio Techniques* 2007; 42:48–58.
23. Gao W, Kondo Y, Shen L, Shimizu Y, Sano T, Yamao K, Natsume A, Goto Y, Ito M, Murakami H, Osada H, Zhang J, et al. Variable DNA methylation patterns associated with progression of disease in hepatocellular carcinomas. *Carcinogenesis* 2008;29:1901–10.
24. Baylin SB, Ohm JE. Epigenetic gene silencing in cancer—a mechanism for early oncogenic pathway addiction? *Nat Rev Cancer* 2006;6:107–16.

25. Estecio MR, Issa JP. Tackling the methylome: recent methodological advances in genome-wide methylation profiling. *Genome Med* 2009;1:106.
26. Mohn F, Schubeler D. Genetics and epigenetics: stability and plasticity during cellular differentiation. *Trends Genet* 2009; 25:129–36.
27. Arase Y, Ikeda K, Suzuki F, Suzuki Y, Kobayashi M, Akuta N, Hosaka T, Sezaki H, Yatsuji H, Kawamura Y, Kobayashi M, Kumada H. Comparison of interferon and lamivudine treatment in Japanese patients with HBeAg positive chronic hepatitis B. *J Med Virol* 2007;79: 1286–92.
28. Yoshida H, Tateishi R, Arakawa Y, Sata M, Fujiyama S, Nishiguchi S, Ishibashi H, Yamada G, Yokosuka O, Shiratori Y, Omata M. Benefit of interferon therapy in hepatocellular carcinoma prevention for individual patients with chronic hepatitis C. *Gut* 2004;53: 425–30.

Published OnlineFirst July 6, 2011; DOI:10.1158/0008-5472.CAN-11-1076

Integrated Systems and Technologies

Cancer Research

Genome-wide Profiling of Chromatin Signatures Reveals Epigenetic Regulation of MicroRNA Genes in Colorectal Cancer

Hiromu Suzuki[1,2], Shintaro Takatsuka[3], Hirofumi Akashi[3], Eiichiro Yamamoto[1,2], Masanori Nojima[4], Reo Maruyama[1], Masahiro Kai[1], Hiro-o Yamano[6], Yasushi Sasaki[5], Takashi Tokino[5], Yasuhisa Shinomura[2], Kohzoh Imai[7], and Minoru Toyota[1]

Abstract

Altered expression of microRNAs (miRNA) occurs commonly in human cancer, but the mechanisms are generally poorly understood. In this study, we examined the contribution of epigenetic mechanisms to miRNA dysregulation in colorectal cancer by carrying out high-resolution ChIP-seq. Specifically, we conducted genome-wide profiling of trimethylated histone H3 lysine 4 (H3K4me3), trimethylated histone H3 lysine 27 (H3K27me3), and dimethylated histone H3 lysine 79 (H3K79me2) in colorectal cancer cell lines. Combining miRNA expression profiles with chromatin signatures enabled us to predict the active promoters of 233 miRNAs encoded in 174 putative primary transcription units. By then comparing miRNA expression and histone modification before and after DNA demethylation, we identified 47 miRNAs encoded in 37 primary transcription units as potential targets of epigenetic silencing. The promoters of 22 transcription units were associated with CpG islands (CGI), all of which were hypermethylated in colorectal cancer cells. DNA demethylation led to increased H3K4me3 marking at silenced miRNA genes, whereas no restoration of H3K79me2 was detected in CGI-methylated miRNA genes. DNA demethylation also led to upregulation of H3K4me3 and H3K27me3 in a number of CGI-methylated miRNA genes. Among the miRNAs we found to be dysregulated, many of which are implicated in human cancer, miR-1-1 was methylated frequently in early and advanced colorectal cancer in which it may act as a tumor suppressor. Our findings offer insight into the association between chromatin signatures and miRNA dysregulation in cancer, and they also suggest that miRNA reexpression may contribute to the effects of epigenetic therapy. *Cancer Res; 71(17); 5646–58. ©2011 AACR.*

Introduction

MicroRNAs (miRNA) are a class of small noncoding RNAs that regulate gene expression by inducing translational inhibition or direct degradation of target mRNAs through base pairing to partially complementary sites (1). miRNA genes are transcribed as large precursor RNAs, called pri-miRNAs, which may encode multiple miRNAs in a polycistronic arrangement. The pri-miRNAs are then processed by the RNase III enzyme Drosha and its cofactor Patha to produce approximately 70-nucleotide hairpin structured second precursors (pre-miRNAs). The pre-miRNAs are then transported to the cytoplasm and processed by another RNase III enzyme, Dicer, to generate mature miRNA products. miRNAs are highly conserved among species and play critical roles in a variety of biological processes, including development, differentiation, cell proliferation, and apoptosis. Subsets of miRNAs are thought to act as tumor suppressor genes (TSG) or oncogenes, and their dysregulation is a common feature of human cancers (2). More specifically, expression of miRNAs is generally downregulated in tumor tissues, as compared with the corresponding normal tissues, which suggests that some miRNAs may behave as TSGs in some tumors. Although the mechanism underlying the alteration of miRNA expression in cancer is still not fully understood, recent studies have shown that multiple mechanisms involved in regulating miRNA levels are affected in cancer. For example, genetic mutations that affect proteins involved in the processing and maturation of miRNA can lead to overall reductions in miRNA expression levels (3, 4). In addition, genetic and epigenetic alterations can disrupt expression of specific miRNAs in cancer.

Authors' Affiliations: [1]Department of Molecular Biology, [2]First Department of Internal Medicine, [3]Scholarly Information Center, [4]Department of Public Health, and [5]Medical Genome Science, Research Institute for Frontier Medicine, Sapporo Medical University, Sapporo; [6]Department of Gastroenterology, Akita Red Cross Hospital, Akita; and [7]Division of Novel Therapy for Cancer, The Advanced Clinical Research Center, The Institute of Medical Science, The University of Tokyo, Tokyo, Japan

Note: Supplementary data for this article are available at Cancer Research Online (http://cancerres.aacrjournals.org/).

Corresponding Author: Hiromu Suzuki, Department of Molecular Biology, Sapporo Medical University, S1, W17, Chuo-Ku, Sapporo 060-8556, Japan. Phone: 81-11-611-2111; Fax: 81-11-622-1918; E-mail: hsuzuki@sapmed.ac.jp

doi: 10.1158/0008-5472.CAN-11-1076

©2011 American Association for Cancer Research.

Downloaded from cancerres.aacrjournals.org on April 26, 2012
Copyright © 2011 American Association for Cancer Research

Published OnlineFirst July 6, 2011; DOI:10.1158/0008-5472.CAN-11-1076

Epigenetic gene silencing due to promoter CpG island (CGI) hypermethylation is one of the most common mechanisms by which TSGs are inactivated during tumorigenesis. In recent years, it has become evident that some miRNA genes are also targets of epigenetic silencing in cancer. Others and we have previously shown that pharmacologic or genetic disruption of DNA methylation in cancer cell lines induces upregulation of substantial numbers of miRNAs (5, 6). These analyses led to identification of candidate tumor-suppressive miRNAs whose silencing was associated with CGI methylation. For example, miR-127 is embedded in a typical CGI, and treatment of human bladder cancer cells with inhibitors of histone deacetylase (HDAC) and DNA methyltransferase (DNMT) induced CGI demethylation and reexpression of the miRNA (7). In addition, methylation of miR-124 family members (miR-124-1, -124-2, and -124-3) was identified in colorectal cancer and was subsequently reported in tumors of other origins (5). Similarly, we found frequent methylation and downregulation of miR-34b/c in both colorectal cancer and gastric cancer (6, 8).

Epigenetic regulation of miRNA genes is tightly linked to chromatin signatures. For instance, transcriptionally active miRNA genes are characterized by active chromatin marks, such as trimethylated histone H3 lysine 4 (H3K4me3; ref. 9). We previously showed that restoring H3K4me3 through DNA demethylation could be a useful marker for predicting the promoter region of a silenced miRNA gene (6). However, the chromatin signatures, including both active and repressive histone marks on miRNA genes, within the cancer genome are still largely unknown. In the present study, we carried out genome-wide profiling of chromatin signatures in colorectal cancer cells and identified the active promoter regions of miRNA genes. We also show that changes in chromatin signatures before and after the removal of DNA methylation lead to robust identification of miRNA genes that are epigenetically regulated in cancer.

Materials and Methods

Cell lines and tissue specimens

Colorectal cancer cell lines and HCT116 cells harboring genetic disruptions within the *DNMT1* and *DNMT3B* loci [double knockout (DKO)] have been described previously (6). Treatment of cells with 5-aza-2′-deoxycytidine (DAC; Sigma-Aldrich) and 4-phenylbutyrate (PBA; Sigma-Aldrich) was carried out as described (8). A total of 90 primary colorectal cancer specimens were obtained as described (6, 10). Samples of adjacent normal colorectal mucosa were also collected from 20 patients. A total of 78 colorectal adenoma specimens were obtained through endoscopic biopsy. Informed consent was obtained from all patients before collection of the specimens. Total RNA from normal colonic mucosa from healthy individuals was purchased from Ambion. Total RNA was extracted using a mirVana miRNA isolation kit (Ambion) or TRIzol reagent (Invitrogen). Genomic DNA was extracted using the standard phenol–chloroform procedure.

miRNA expression profiling

Expression of 470 miRNAs was analyzed using Human miRNA Microarray VI (G4470A; Agilent Technologies) as described previously (8). In addition, expression of 664 miRNAs was analyzed using a TaqMan microRNA Array v2.0 (Applied Biosystems). Briefly, 1 μg of total RNA was reverse transcribed using Megaplex Pools kit (Applied Biosystems), after which the miRNAs were amplified and detected using PCR with specific primers and TaqMan probes. The PCR was run in a 7900HT Fast Real-Time PCR system (Applied Biosystems), and SDS2.2.2 software (Applied Biosystems) was used for comparative ΔC_t analysis. U6 snRNA (RNU6B; Applied Biosystems) served as an endogenous control. Microarray data and TaqMan Array data (ΔC_t values) were further analyzed using GeneSpring GX ver. 11 (Agilent Technologies). The Gene Expression Omnibus accession number for the microarray data is GSE29900.

Real-time reverse transcriptase PCR of miRNA

Expression of selected miRNAs was analyzed using TaqMan microRNA Assays (Applied Biosystems). Briefly, 5 ng of total RNA was reverse transcribed using specific stem-loop RT primers, after which the miRNAs were amplified and detected using PCR with specific primers and TaqMan probes as described earlier. U6 snRNA (RNU6B) served as an endogenous control. Expression of the primary miR-1-1 transcript was analyzed using a TaqMan Pri-miRNA assay (assay ID Hs03303345_pri; Applied Biosystems). Glyceraldehyde-3-phosphate dehydrogenase (GAPDH; assay ID Hs99999905_m1; Applied Biosystems) served as an endogenous control.

Chromatin immunoprecipitation-on-chip analysis

Chromatin immunoprecipitation (ChIP)-on-chip analysis was carried out according to Agilent Mammalian ChIP-on-chip Protocol version 10.0 (Agilent Technologies). Briefly, 1×10^8 cells were treated with 1% formaldehyde for 10 minutes to cross-link histones with the DNA. After washing with PBS, the cell pellets were resuspended in 3 mL of lysis buffer and sonicated. Chromatin was immunoprecipitated for 16 hours at 4°C using 10 μL of anti-trimethyl histone H3K4 (clone MC315; Upstate), anti-trimethyl histone (clone H3K27; Upstate) or anti-dimethyl histone H3K79 (clone NL59; Upstate) antibody. Before adding antibodies, 50 μL of the each cell lysate was saved as an internal control for the input DNA. After washing, elution, and reversal of the cross-links, input DNA and the immunoprecipitate were ligated to linkers and PCR amplified. Input DNA and the immunoprecipitate were then labeled with Cy3 and Cy5 using an Agilent Genomic DNA Enzymatic Labeling kit (Agilent Technologies) and hybridized to the 244K Human Promoter ChIP-on-chip microarray (G4489A; Agilent technologies). After washing, the array was scanned using an Agilent DNA Microarray scanner (Agilent Technologies), and the data were processed using Feature Extraction software (Agilent Technologies).

ChIP-seq analysis

ChIP experiments were carried out as described earlier, after which massively parallel sequencing was carried out

Downloaded from cancerres.aacrjournals.org on April 26, 2012
Copyright © 2011 American Association for Cancer Research

Published OnlineFirst July 6, 2011; DOI:10.1158/0008-5472.CAN-11-1076

using a SOLiD3 Plus system (Applied Biosystems) according to the manufacturer's instructions. Briefly, 100 ng of input DNA or the immunoprecipitate was ligated to adapters and PCR amplified using a SOLiD Fragment Library Construction kit (Applied Biosystems). Template bead preparation was carried out using a SOLiD ePCR kit V2 (Applied Biosystems) and a SOLiD Bead Enrichment kit (Applied Biosystems). Approximately 40 to 50 million beads per sample were sequenced using SOLiD Opti Fragment Library Sequencing Master Mix 50 (Applied Biosystems) and a SOLiD3 Plus sequencer (Applied Biosystems). Sequence reads that were of poor quality or those that were not uniquely mapped were excluded from the study. Peaks were identified using the Model-based Analysis for ChIP-seq (MACS) software (11) and visualized using the University of California Santa Cruz (UCSC) genome browser.

Reference sequence

Genomic locations are based on the UCSC hg18 (National Center for Biotechnology Information Build 36.1, March 2006), which was produced by the International Human Genome Sequencing Consortium. We also obtained locations of CGIs, ReSeq genes, and UCSC genes from the UCSC hg18 data sets.

Methylation analysis

Genomic DNA (2 μg) was modified with sodium bisulfite using an EpiTect Bisulfite kit (QIAGEN). Methylation-specific PCR (MSP), bisulfite sequencing, and bisulfite pyrosequencing were carried out as described (6). For bisulfite sequencing analysis, amplified PCR products were cloned into pCR2.1-TOPO vector (Invitrogen), and 10 to 12 clones from each sample were sequenced using an ABI3130x automated sequencer (Applied Biosystems). Primer sequences and PCR product sizes are listed in Supplementary Table S1.

Transfection of miRNA precursor molecules

Colorectal cancer cells (1×10^6 cells) were transfected with 100 pmol of Pre-miR miRNA Precursor Molecules (Ambion) or Pre-miR miRNA Molecules Negative Control #1 (Ambion) using a Cell Line Nucleofector kit V (Lonza) with a Nucleofector I electroporation device (Lonza) according to the manufacturer's instructions. Total RNA or cell lysate was extracted 48 hours after transfection. Cell viability assays, Western blotting, wound-healing assays, and Matrigel invasion assays are described in the Supplementary Methods..

Gene expression profiling

Total RNA (700 ng) was amplified and labeled using a Quick Amp Labeling kit one-color (Agilent Technologies), after which the synthesized cRNA was hybridized to the Whole Human Genome Oligo DNA microarray (G4112F; Agilent technologies). Data analysis was carried out using GeneSpring GX ver. 11 (Agilent technologies). The Gene Expression Omnibus accession number for the microarray data is GSE29760.

miRNA target predictions and luciferase reporter assays

The predicted targets of miR-1 and their downstream target sites were analyzed using TargetScan and miRanda. Construction of luciferase reporter vectors containing the predicted target sites and dual luciferase reporter assays were carried out as described in Supplementary Methods.

Results

miRNA profiling in colorectal cancer cell lines

To screen for epigenetically silenced miRNAs, we first carried out miRNA microarray analysis in a series of colorectal cancer cell lines (HCT116, DLD1, and RKO) and normal colonic tissue. Hierarchical clustering analysis revealed that expression of a majority of miRNAs was downregulated in all 3 colorectal cancer cell lines tested, as compared with normal colonic mucosa (Supplementary Fig. S1A). DAC treatment upregulated expression of a large number of miRNAs in all 3 colorectal cancer cell lines (Supplementary Fig. S1B), and combination treatment with DAC plus PBA induced even greater numbers of miRNAs in colorectal cancer cells (Supplementary Fig. S1C and D). However, the most profound effect on the miRNA expression profile was induced by genetic disruption of *DNMT1* and *DNMT3B* in HCT116 cells (DKO cells; Supplementary Fig. S1C). We also noted a novel overlap between miRNAs upregulated by pharmacologic or genetic disruption of DNA methylation and those downregulated in colorectal cancer cells, as compared with normal colonic mucosa (Supplementary Fig. S1E–G). To test the tumor-suppressive potentials of the downregulated miRNAs, we constructed expression vectors encoding selected miRNAs and carried out colony formation assays. We found that a majority of miRNAs exerted growth-suppressive effects when they were ectopically expressed in colorectal cancer cells (Supplementary Fig. S2). These results suggest that an epigenetic mechanism plays an essential role in the downregulation of a number of miRNAs in cancer and that such downregulation of numerous miRNAs may contribute to tumorigenesis.

Chromatin signatures of active and silenced miRNA genes

We next examined the chromatin signatures of miRNA genes in HCT116 colorectal cancer cells, with and without genetic disruption of *DNMT1* and *DNMT3B* (DKO cells). We carried out ChIP analysis using antibodies against trimethylated histone H3 lysine 4 (H3K4me3), which marks active promoters; dimethylated histone H3 lysine 79 (H3K79me2), which is associated with transcriptional elongation; and trimethylated histone H3 lysine 27 (H3K27me3), which is a repressive mark. We started our analysis using the Agilent 244K Promoter Array, which covers approximately 370 human miRNA genes, and we subsequently migrated to ChIP-seq analysis to increase our scope within the genome. We observed a good correlation between the results of the ChIP-on-chip and ChIP-seq analyses (Supplementary Fig. S3). We also validated the reliability of our ChIP-seq data by checking representative protein-coding genes that were transcriptionally active or silenced in HCT116 cells (Supplementary Fig. S4).

Representative chromatin signatures of miRNA genes are shown in Fig. 1A. We found enrichment of the H3K4me3 mark around the proximal upstream CGI regions of 2 abundantly

Downloaded from cancerres.aacrjournals.org on April 26, 2012
Copyright © 2011 American Association for Cancer Research

Published OnlineFirst July 6, 2011; DOI:10.1158/0008-5472.CAN-11-1076

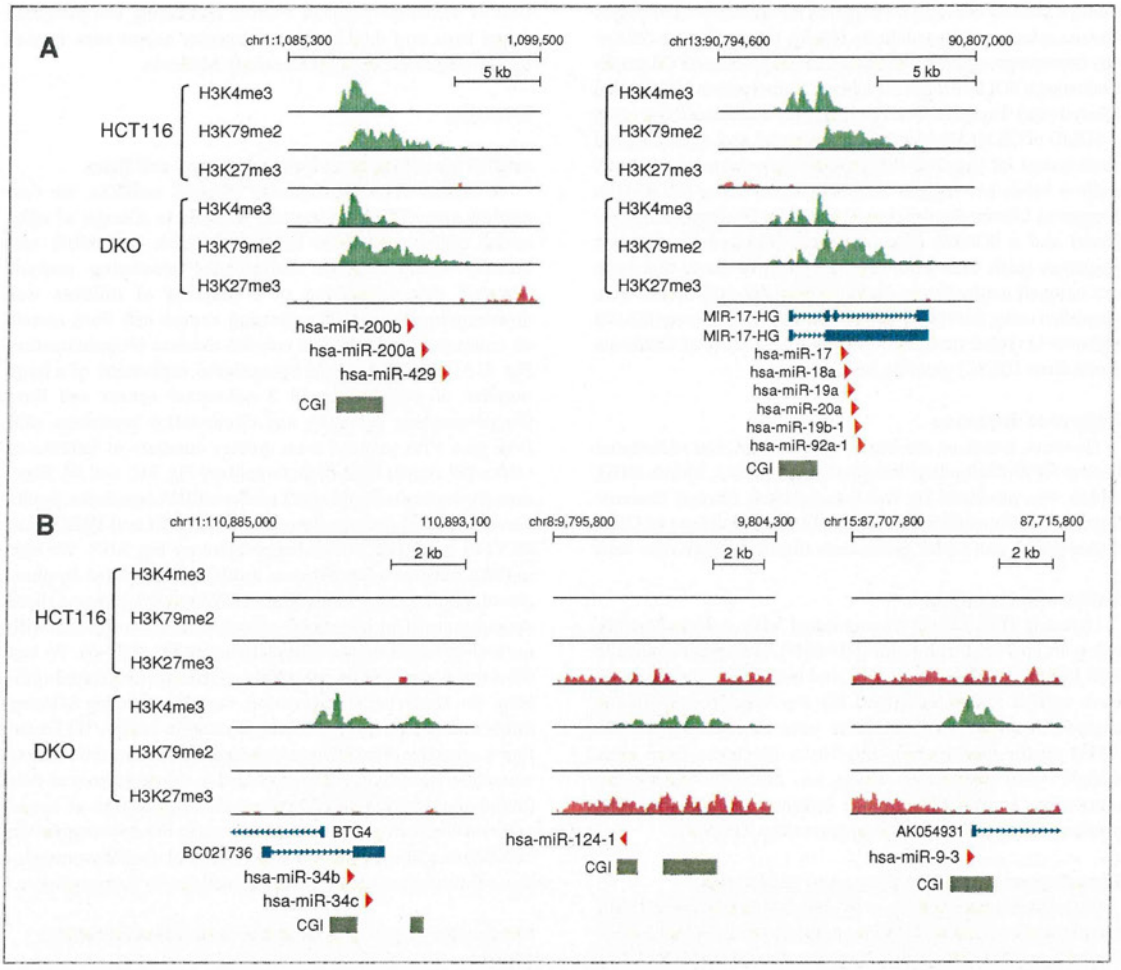

Figure 1. Chromatin signatures of transcriptionally active and epigenetically silenced miRNA genes in colorectal cancer. A, ChIP-seq results for H3K4me3, H3K79me2, and H3K27me3 in transcriptionally active miRNA genes in HCT116 and DKO cells. Chromosomal locations are indicated on the top. Locations of host genes, pre-miRNA genes, and CGIs are shown below. B, ChIP-seq results for epigenetically silenced miRNAs with associated CGI hypermethylation. CGI methylation is lost and miRNAs are reexpressed in DKO cells. H3K4me3 marking is upregulated in the putative promoter regions in DKO cells, whereas H3K79me2 shows only a minimal increase.

expressed miRNA clusters, miR-200b and miR-17, in both wild-type HCT116 and DKO cells (Fig. 1A). Gene bodies were marked by H3K79me2, which indicates active transcriptional elongation, whereas they almost completely lacked the repressive H3K27me3 mark. With respect to the H3K4me3 mark in the miR-17 cluster, we observed a sharp dip at the transcription start site (TSS) of the host gene and another dip downstream, which is consistent with a previous report that miR-17 has its own TSS within the intron of the host gene (Fig. 1A; ref. 12).

In contrast, miRNAs whose silencing was associated with promoter CGI hypermethylation completely lacked both of the active histone marks. The CGIs of miR-34b/c, miR-124-1, and miR-9-3 were densely methylated in HCT116 cells (5, 6, 13) and were completely devoid of H3K4me3 and H3K79me2 marks (Fig. 1B). miR-124-1 and miR-9-3 showed moderate enrichment of H3K27me3, whereas miR-34b/c was almost H3K27me3 free, which corresponds to previous reports that DNA methylation and H3K27me3 are sometimes observed independently in cancer (14). In DKO cells, where DNA methylation was significantly diminished and gene expression was restored, increased H3K4me3 marks were found at the upstream CGI, though restoration of H3K79me2 was quite limited. Upregulation of H3K27me3 was also seen around miR-124-1 and miR-9-3, which is consistent with previous observations that genes with methylated CGIs adopt a bivalent chromatin pattern after DNA demethylation (15, 16).

Downloaded from cancerres.aacrjournals.org on April 26, 2012
Copyright © 2011 American Association for Cancer Research

Published OnlineFirst July 6, 2011; DOI:10.1158/0008-5472.CAN-11-1076

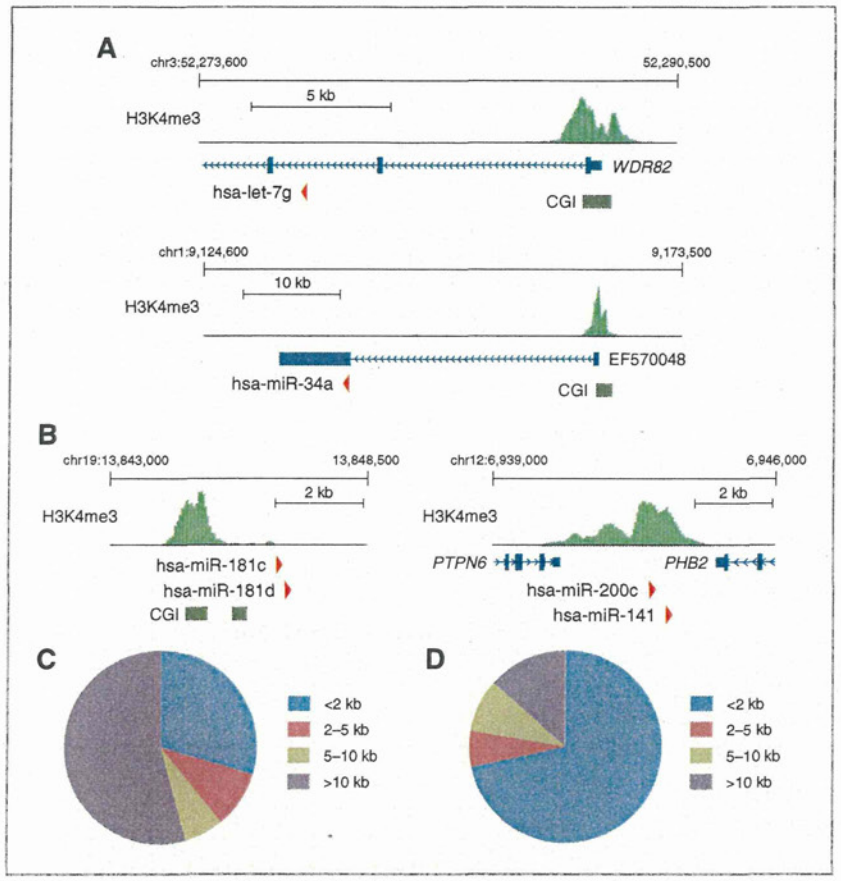

Figure 2. Identification of miRNA gene promoter regions using chromatin signatures. A, examples of H3K4me3 marks in intragenic miRNAs. Let-7g is located within the intron of the protein-coding gene *WDR82*, and miR-34a is located within the exon of a noncoding host gene. H3K4me3 marks are observed in the TSS regions of the host genes, suggesting that these miRNAs share common promoters with their host genes. B, examples of H3K4me3 marking of intergenic miRNA genes. C, summarized distances between intragenic pre-miRNA coding regions and their putative promoter regions (n = 166). D, summarized distances between intergenic pre-miRNA coding regions and their putative promoter regions (n = 67).

Identification of putative miRNA promoter regions

Identification of epigenetically silenced miRNAs is sometimes hampered by a lack of knowledge of the transcription initiation region of the primary miRNA transcripts. Previous studies have shown that H3K4me3 is a useful marker for identifying active miRNA gene promoters (9, 12), and we employed that approach with colorectal cancer cells. Using miRNA microarrays and TaqMan low-density arrays, we detected expression of 339 and 429 distinct mature miRNAs in HCT116 and DKO cells, respectively. We then searched for the putative promoter regions of these miRNAs, using H3K4me3 as a marker.

More than half of miRNAs are located in the introns of protein-coding or long noncoding RNA genes, and it is generally believed that intragenic miRNAs share common promoters with their host genes (17). We identified the putative promoters of 166 intragenic miRNAs located in RefSeq genes and/or UCSC genes, and a majority of the H3K4me3 marks were observed at the TSS of the host genes, many of which were located more than 10 kb upstream of the pre-miRNA coding regions (Fig. 2A and C, Supplementary Fig. S5A, and Supplementary Table S2). In contrast, intragenic H3K4me3 marks were identified in the proximal upstream of 22 pre-miRNAs, indicating these miRNAs have their own promoters and are transcribed independently of their host genes (Supplementary Fig. S6, Supplementary Table S3). To identify promoters of intergenic miRNAs, we first searched 10 kb upstream for H3K4me3 marks and also explored the initiation sites of overlapping 5′ expressed sequence tags (EST). We identified the putative promoters of 66 intergenic miRNAs, the majority of which (47 of 66) were identified in the proximal upstream (<2 kb) of the pre-miRNA coding region (Fig. 2B and D, Supplementary Fig. S5B, and Supplementary Table S2). In total, we identified the putative promoters of 174 transcript units encoding 233 distinct pre-miRNAs, whereas promoters of 135 miRNAs remain unidentified, despite their positive expression in colorectal cancer cells.

We validated our promoter search by comparing our results with previously reported transcription initiation regions. Promoters of 177 pre-miRNAs that we identified overlapped with those identified in human embryonic stem (ES) cells by Marson and colleagues (9), whereas only the promoters of 38 pre-miRNAs did not match. Similarly, the TSS of 65 miRNAs identified in human melanoma and breast cancer cell lines by

Downloaded from cancerres.aacrjournals.org on April 26, 2012
Copyright © 2011 American Association for Cancer Research

Published OnlineFirst July 6, 2011; DOI:10.1158/0008-5472.CAN-11-1076

Ozsolak and colleagues overlapped with the promoters we identified (12). For example, we found H3K4me3 marks overlapping with known TSS of the miR-17 cluster, let-7a-1/let-7f-1/let-7d, and miR-200c/141 (Fig. 2B, Supplementary Fig. S5). We also identified an H3K4me3 mark at the intronic transcription initiating region of miR-21 (Supplementary Fig. S6C). The high degree of consistency between our results and those of earlier studies attests to the accuracy of our promoter prediction.

Identification of epigenetically silenced miRNAs

We next endeavored to identify epigenetically silenced miRNA genes by taking advantage of the observation that DNA demethylation can induce increases in H3K4me3 in the promoters of the epigenetically silenced genes (6). We searched for miRNA genes showing reduction or loss of both expression and H3K4me3 marks in HCT116 and DKO cells. We identified 47 pre-miRNA genes encoded in 37 primary transcription units as potential targets of epigenetic silencing in HCT116 cells. Promoters of 22 transcription units were associated with CGIs, and MSP analysis revealed that all of the CGIs were methylated (Fig. 3A and B, Table 1). In most cases, DNA demethylation led to increases in H3K4me3 and H3K27me3 marking of the methylated CGIs of miRNA genes, whereas H3K79me2 marks were not restored by demethylation (Fig. 3C). In contrast, the chromatin signatures of miRNAs without promoter CGIs were more variable among genes. We

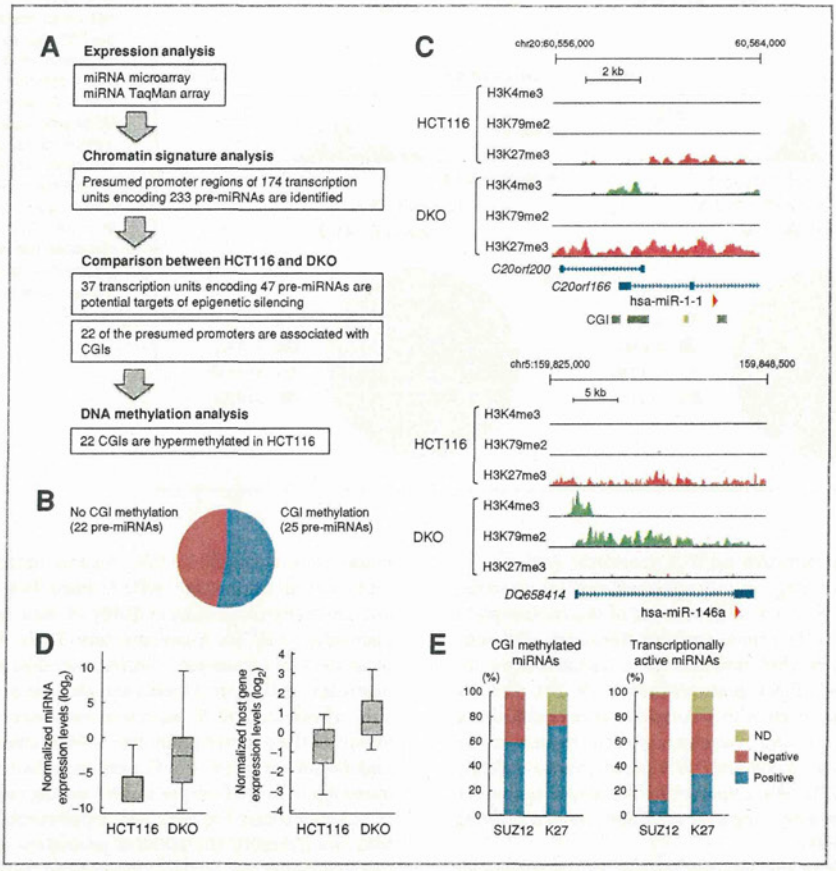

Figure 3. Identification of epigenetically silenced miRNA genes. A, flowchart for the selection of epigenetically silenced miRNA genes in colorectal cancer. B, graph showing the number of epigenetically silenced miRNAs associated with CGI methylation and those without CGI methylation. C, chromatin signatures of 2 representative miRNA genes, with and without promoter CGI methylation. miR-1-1 (top) was silenced in association with CGI methylation in HCT116 cells. In DKO cells, H3K4me3 marking was observed around the transcription start site of the host gene *C20orf166*. miR-146a (bottom) is another candidate target for epigenetic silencing in HCT116, though its promoter is not associated with CGI. Both H4K4me3 and H3K79me2 were restored in DKO cells. D, expression levels of epigenetically silenced miRNAs and their host genes in HCT116 and DKO cells. TaqMan real-time PCR data for 57 mature miRNAs encoded by 47 pre-miRNA genes were imported into Gene Spring GX, after which the data were normalized and shown in box plots (left). Expression data of 13 host genes of epigenetically silenced miRNAs were obtained using an Agilent Whole Human Genome microarray (right). E, miRNAs targeted by the PcG group in ES cells are more likely to be silenced by CGI hypermethylation in colorectal cancer cells. CGI-methylated miRNAs ($n = 22$; left) or transcriptionally active miRNAs ($n = 146$; right) were selected, and their SUZ12 binding and H3K27me3 enrichment in human ES cells were assessed. Of 22 CGI-methylated miRNAs, 13 (59%) were positive for SUZ12 and 16 (73%) for H3K27me3. ND, not determined.

Downloaded from cancerres.aacrjournals.org on April 26, 2012
Copyright © 2011 American Association for Cancer Research

Published OnlineFirst July 6, 2011; DOI:10.1158/0008-5472.CAN-11-1076

Table 1. Epigenetically silenced miRNA genes in HCT116

Name	miRNA position	Strand	Gene/EST	DKO H3K4me3	Distance	CpG	Methylation
hsa-mir-137	chr1:98284213-98284315	–	*AK311400*	chr1:98282607-98285011	<2 kb	CGI	M
hsa-mir-488	chr1:175265121-175265204	–	*ASTN1*	chr1:175267182-175269163	<2 kb	–	
hsa-mir-205	chr1:207672100-207672210	+	*LOC642587*	chr1:207668045-207668780	2–5 kb	–	
hsa-mir-10b	chr2:176723276-176723386		EST: BQ722165	chr2:176720798-176721389	<2 kb	CGI	M
hsa-mir-885	chr3:10411172-10411246	–	*ATP2B2*	chr3:10723790-10724643	>10 kb	–	
hsa-mir-944	chr3:191030404-191030492	+	*TP63*	chr3:190831254-190831806	>10 kb	–	
hsa-mir-146a	chr5:159844936-159845035	+	*DQ658414*	chr5:159827186-159829843	>10 kb	–	
hsa-mir-218-2	chr5:168127728-168127838	–	*SLIT3*	chr5:168127234-168128479	<2 kb	–	
hsa-mir-9-2	chr5:87998426-87998513	–	*LOC645323*	chr5:87997315-87999774	<2 kb	–	
hsa-mir-548b	chr6:119431910-119432007	–	*FAM184A*	chr6:119440287-119442581	5–10 kb	CGI	M
hsa-mir-129-1	chr7:127635160-127635232	+		chr7:127628134-127629349	5–10 kb	CGI	M
hsa-mir-153-2	chr7:157059788-157059875	–	*PTPRN2*	chr7:157061089-157064064	<2 kb	CGI	M
hsa-mir-596	chr8:1752803-1752880	+		chr8:1751984-1754090	<2 kb	CGI	M
hsa-mir-124-1	chr8:9798307-9798392	–		chr8:9798198-9799439	<2 kb	CGI	M
hsa-mir-598	chr8:10930125-10930222	–	*XKR6*	chr8:11094125-11097386	>10 kb	CGI	M
hsa-mir-486	chr8:41637115-41637183	–	*ANK1*	chr8:41660039-41661630	>10 kb	–	
hsa-mir-124-2	chr8:65454259-65454368	+	*BX537900*	chr8:65452660-65453362	<2 kb	CGI	M
hsa-mir-876	chr9:28853623-28853704	–	EST: DA506041	chr9:29200954-29205760	>10 kb	CGI	M
hsa-mir-873	chr9:28878876-28878953	–	EST: DA506041	chr9:29200954-29205760	>10 kb	CGI	M
hsa-mir-146b	chr10:104186258-104186331	+		chr10:104185067-104186052	<2 kb	–	
hsa-mir-129-2	chr11:43559519-43559609	+	EST: BI964058	chr11:43556836-43561086	<2 kb	CGI	M
hsa-mir-708	chr11:78790713-78790801	–	*ODZ4*	chr11:78825491-78830366	>10 kb	CGI	M
hsa-mir-34b	chr11:110888872-110888956	+	*BC021736*	chr11:110887701-110889527	<2 kb	CGI	M
hsa-mir-34c	chr11:110889373-110889450	+	*BC021736*	chr11:110887701-110889527	<2 kb	CGI	M
hsa-mir-337	chr14:100410582-100410675	+		chr14:100407328-100408197	2–5 kb	–	
hsa-mir-431	chr14:100417096-100417210	+		chr14:100417110-100420818	<2 kb	–	
hsa-mir-433	chr14:100417975-100418068	+		chr14:100417110-100420818	<2 kb	–	
hsa-mir-127	chr14:100419068-100419165	+		chr14:100417110-100420818	<2 kb	CGI	M
hsa-mir-432	chr14:100420572-100420666	+		chr14:100417110-100420818	<2 kb	–	
hsa-mir-136	chr14:100420791-100420873	+		chr14:100417110-100420818	<2 kb	–	
hsa-mir-211	chr15:29144526-29144636	–	*TRPM1*	chr15:29160209-29160816	>10 kb	–	
hsa-mir-190	chr15:60903208-60903293	+	*TLN2*	chr15:60769608-60770528	>10 kb	–	
hsa-mir-9-3	chr15:87712251-87712341	+	*CR612213*	chr15:87711049-87714084	<2 kb	CGI	M
hsa-mir-195	chr17:6861657-6861744	–	EST: DA285925	chr17:6862382-6864312	<2 kb	–	
hsa-mir-497	chr17:6861953-6862065	–	EST: DA285925	chr17:6862382-6864312	<2 kb	–	
hsa-mir-193a	chr17:26911127-26911215	+		chr17:26910360-26912430	<2 kb	CGI	M
hsa-mir-152	chr17:43469525-43469612	–	*COPZ2*	chr17:43468887-43470981	<2 kb	CGI	M
hsa-mir-196a-1	chr17:44064850-44064920	–	EST:AI222881	chr17:44065082-44066831	<2 kb	CGI	M
hsa-mir-142	chr17:53763591-53763678	–	*AK311311* (antisense)	chr17:53762545-53765705	<2 kb	–	
hsa-mir-338	chr17:76714277-76714344	–	*AATK*	chr17:76753247-76754663	>10 kb	CGI	M
hsa-mir-371	chr19:58982740-58982807	+		chr19:58982297-58983364	<2 kb	–	
hsa-mir-372	chr19:58982955-58983022	+		chr19:58982297-58983364	<2 kb	–	
hsa-mir-373	chr19:58983770-58983839	+		chr19:58982297-58983364	<2 kb	–	
hsa-mir-1-1	chr20:60561957-60562028	+	*C20orf166*	chr20:60557701-60559681	2–5 kb	CGI	M
hsa-mir-133a-2	chr20:60572563-60572665	+	*C20orf166*	chr20:60557701-60559681	>10 kb	CGI	M
hsa-mir-124-3	chr20:61280296-61280383	+		chr20:61276185-61277804	2–5 kb	CGI	M
hsa-mir-155	chr21:25868162-25868227	+	*MIR155HG*	chr21:25855844-25857551	>10 kb	CGI	M

Abbreviations: gene/EST, overlapping gene or EST; distance, distance between pre-miRNA coding region and presumed promoter; CGI, CpG island positive at the promoter; M, CGI methylated.

Downloaded from cancerres.aacrjournals.org on April 26, 2012
Copyright © 2011 American Association for Cancer Research

Published OnlineFirst July 6, 2011; DOI:10.1158/0008-5472.CAN-11-1076

noted that a small number of non-CGI miRNAs acquired more active chromatin states upon DNA demethylation than did CGI-methylated miRNAs. For instance, miR-146a is characterized by a lack of active histone marks and enrichment of H3K27me3, but it showed restoration of both H3K4me3 and H3K79me2 in DKO cells (Fig. 3C). We observed similar upregulation of both active marks in miR-142 (Supplementary Fig. S7E). Weak basal expression of these miRNAs, detectable by TaqMan assay but not by microarray, and robust upregulation after DNA demethylation indicate that the silencing of these miRNAs is less stringent than that of miRNAs with methylated CGIs (data not shown).

DNA demethylation significantly upregulated the expression of mature miRNAs derived from 47 silenced pre-miRNAs (Fig. 3D). In addition, expression data from 13 host genes of the silenced miRNAs were obtained from Agilent gene expression microarray analysis (6), and we observed a strong tendency for the host genes to be upregulated by DNA demethylation (Fig. 3E). Recent studies have shown that genes marked by polycomb (PcG) group proteins in ES cells have a predisposition toward DNA hypermethylation in cancer (18, 19). By comparison with previously published results (9), we found that miRNAs with SUZ12 binding and H3K27me3 marks in human ES cells are significantly enriched in CGI-methylated miRNAs in colorectal cancer (Fig. 3E).

We further analyzed CGI methylation in a series of colorectal cancer cell lines using MSP and bisulfite pyrosequencing and found that they are methylated to varying degrees (Fig. 4A, Supplementary Fig. S8). We also confirmed inverse relationships between methylation and expression of selected miRNAs in colorectal cancer cell lines and normal colonic tissue (Fig. 4B). To determine the extent to which these miRNA genes are aberrantly methylated in primary tumors, we carried out bisulfite pyrosequencing of 18 miRNA promoter CGIs in primary colorectal cancer tumors ($n = 90$) and normal colonic tissue obtained from colorectal cancer patients ($n = 20$; Supplementary Fig. S9). Most of the miRNA genes were methylated in a tumor-specific or tumor-predominant manner. The two exceptions were miR-153-2 and miR-196a-1, which were methylated to similar degrees in both normal colon and tumor tissues, as well as in various normal human tissues (Supplementary Figs. S9 and S10). Elevated levels of miRNA gene methylation (>15.0%) were frequently detected in primary colorectal cancer tumors (miR-1-1, 77.8%; miR-9-1, 57.8%; miR-9-3, 89.9%; miR-34b/c, 89.7%; miR-124-1, 87.7%: miR-124-2, 96.6%; miR-124-3, 100.0%; miR-128-2, 73.6%; miR-129-2, 40.0%; miR-137, 100.0%; miR-193a, 28.7%; miR-338, 15.6%; and miR-548b, 47.8%), whereas a small number of genes were rarely methylated in primary tumors (miR-152, 4.4%; miR-155, 6.7%; and miR-596, 2.3%).

MiR-1-1 is a candidate tumor suppressor gene in colorectal cancer

Among the epigenetically silenced miRNAs, we next focused on miR-1-1 because it has received relatively little attention in colorectal cancer despite its frequent hypermethylation in that disease. Using bisulfite pyrosequencing, we detected elevated levels (>15.0%) of miR-1-1 methylation in both primary colorectal cancer tumors and colorectal adenomas (54 of 78, 69.2%), suggesting that its methylation is an early event in colorectal tumorigenesis (Fig. 5A). In contrast, levels of miR-1-1 methylation were relatively low (<15.0%) in the normal colonic tissues tested (Fig. 5A). We carried out bisulfite sequencing analysis to confirm the methylation results in selected tissue specimens and colorectal cancer cell lines (Fig. 5B, Supplementary Fig. S11A and B). We also confirmed that DNA demethylation could restore expression of the primary transcript of miR-1-1 (pri-miR-1-1) in colorectal cancer cells (Supplementary Fig. S11C).

To determine whether miR-1-1 serves as a tumor suppressor in colorectal cancer, we transfected colorectal cancer cell lines with a miR-1 precursor molecule or a negative control and then carried out a series of MTT assays. Forty-eight hours after transfection, we observed that ectopic expression of miR-1 moderately suppressed growth in all 3 cell lines (Fig. 5C). Colony formation assays also revealed reduced colony formation by colorectal cancer cells transfected with a miR-1-1 expression vector (Fig. 5D).

To further clarify the effect of the miRNA, we next carried out a gene expression microarray analysis of HCT116 cells transfected with a miR-1 precursor molecule or a negative control. We found that 2,769 probe sets were downregulated (>1.5-fold) by ectopic miR-1 expression, and gene ontology analysis revealed that "extracellular regions," "membrane," and "response to wounding" genes were significantly enriched among the downregulated genes (Supplementary Table S4). The genes downregulated by miR-1 included a number of predicted miR-1 targets (Supplementary Table S5). Among them, we noted 2 genes, Annexin A2 (*ANXA2*) and brain-derived neurotrophic factor (*BDNF*), which have been implicated in tumor growth and metastasis (20–22). Reduction of their expression by miR-1 in colorectal cancer cells was confirmed by Western blotting and real-time reverse transcriptase PCR (RT-PCR; Fig. 5E, Supplementary Fig. S12A). Reporter assays using luciferase vectors containing the putative miR-1 binding sites revealed that cotransfection of a miR-1 precursor molecule markedly reduced luciferase activities and that such reductions were not induced by a negative control or an irrelevant miRNA molecule (Fig. 5F and G, Supplementary Fig. S12B and S12C). Finally, we carried out wound-healing and Matrigel invasion assays to test the effect of miR-1 expression on colorectal cancer cell migration and invasion. We found that wound closure by HCT116 cells transfected with the negative control was complete within 28 hours whereas miR-1–expressing cells migrated toward the wound at a much slower rate (Fig. 5H). We also observed significant inhibition of cell invasion by miR-1 in HCT116 cells (Fig. 5I). These results strongly suggest that miR-1 acts as a tumor suppressor in colorectal cancer.

Discussion

In the present study, we provide a comprehensive view of the epigenetic regulation of miRNA genes in colorectal cancer cells. Because of the poor annotation of primary miRNA genes, the precise locations of the promoters and TSSs are not fully understood yet. To overcome these difficulties, earlier studies have searched for specific genomic features including RNA

Downloaded from cancerres.aacrjournals.org on April 26, 2012
Copyright © 2011 American Association for Cancer Research

Published OnlineFirst July 6, 2011; DOI:10.1158/0008-5472.CAN-11-1076

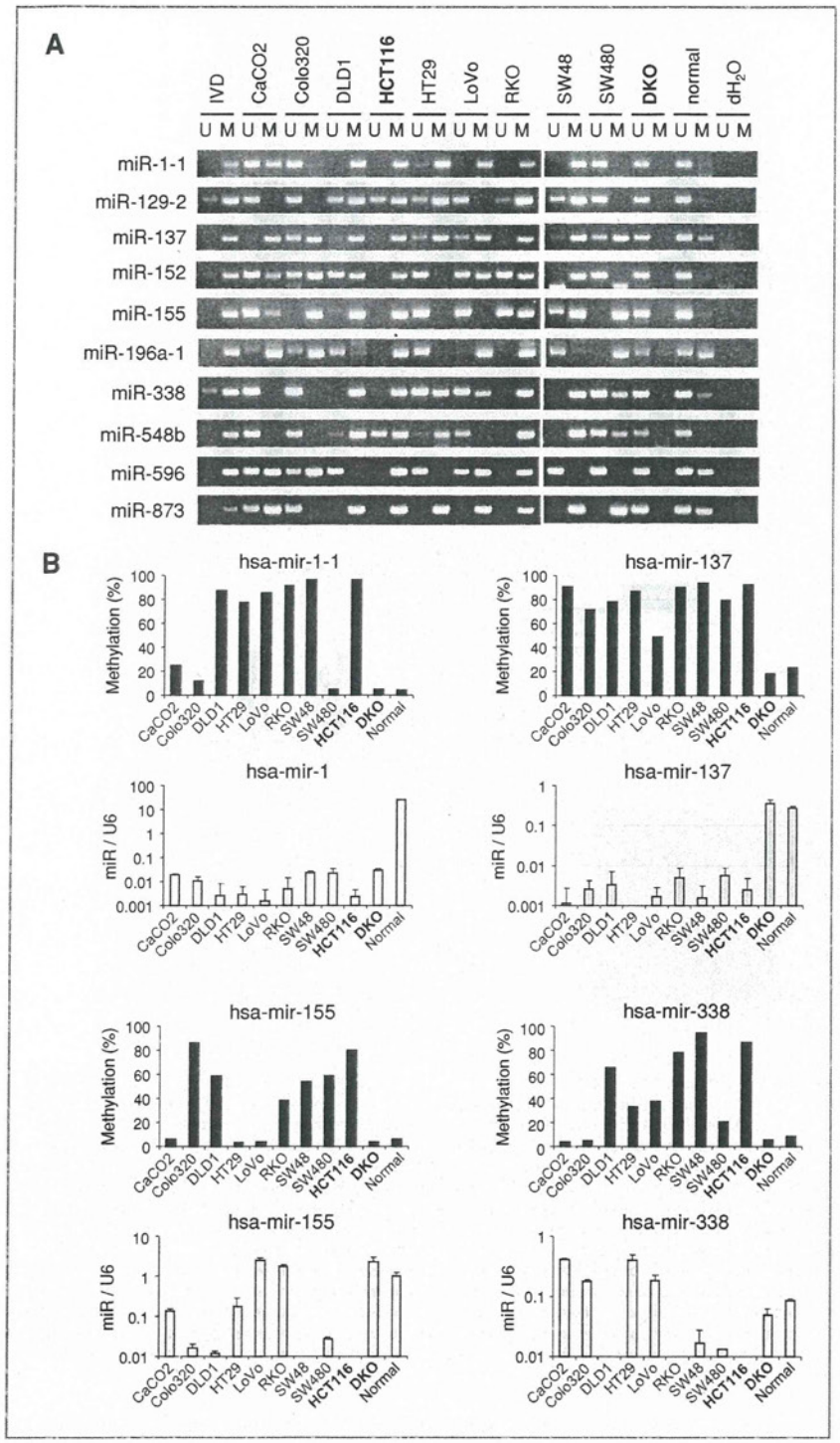

Figure 4. DNA methylation and expression analysis of miRNAs in colorectal cancer cells. A, representative results of MSP analysis of a series of colorectal cancer cell lines and normal colonic tissue. Bands in the "M" lanes are PCR products obtained with methylation-specific primers; those in the "U" lanes are products obtained with unmethylated-specific primers. *In vitro* methylated DNA (IVD) serves as a positive control. B, relationship between DNA methylation and expression of miRNAs in colorectal cancer. Bisulfite pyrosequencing results for miRNA promoter CGIs (black bars) and TaqMan real-time PCR results for mature miRNAs (gray bars) in a series of colorectal cancer cell lines and normal colonic tissue are shown. RT-PCR results were normalized to internal U6 snRNA expression.

Downloaded from cancerres.aacrjournals.org on April 26, 2012
Copyright © 2011 American Association for Cancer Research

Published OnlineFirst July 6, 2011; DOI:10.1158/0008-5472.CAN-11-1076

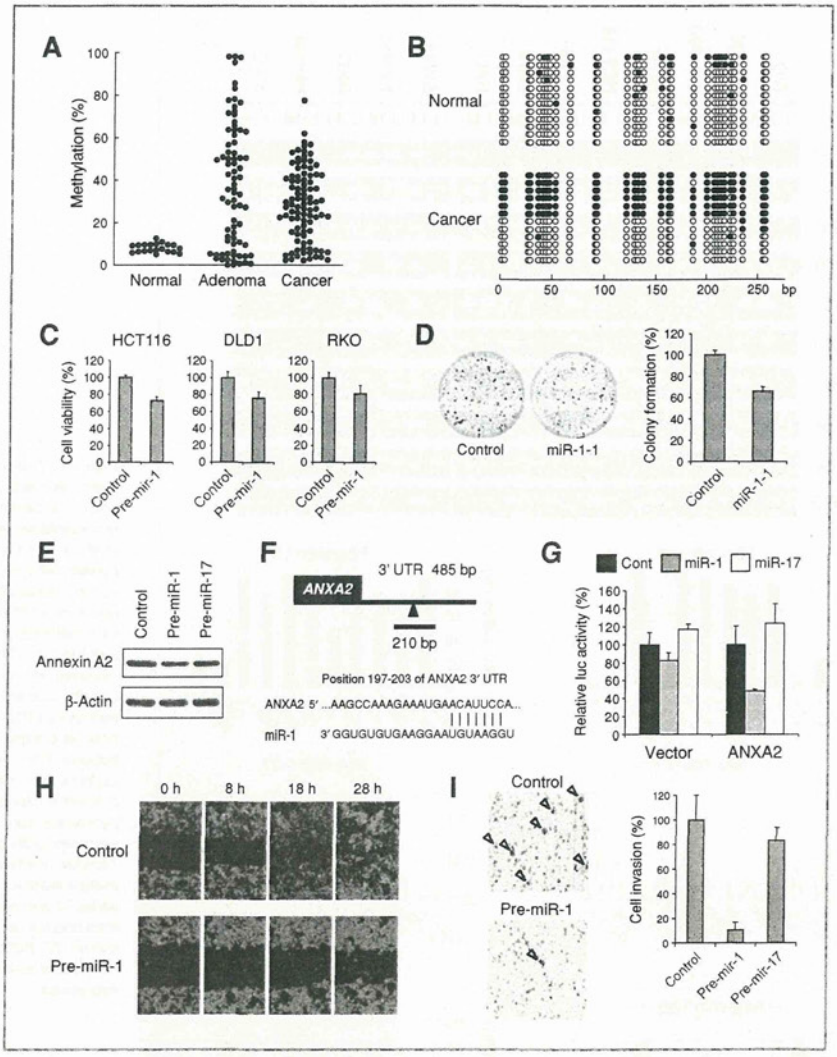

Figure 5. Methylation and functional analysis of miR-1-1 in colorectal cancer. A, summarized bisulfite pyrosequencing results for the miR-1-1 promoter CGI in normal colonic tissue ($n = 20$), colorectal adenomas ($n = 78$), and primary colorectal cancer tumors ($n = 90$). B, representative bisulfite sequencing results for the miR-1-1 promoter in a sample of normal colonic tissue and a primary colorectal cancer tumor. Open and filled circles represent unmethylated and methylated CpG sites, respectively. C, MTT assays with colorectal cancer cell lines transfected with a miR-1 precursor molecule or a negative control. Cell viabilities were determined 48 hours after transfection. Values were normalized to cells transfected with the negative control. Shown are the means of 8 replications; error bars represent SDs. D, colony formation assays using HCT116 cells transfected with a miR-1-1 expression vector or a control vector. Representative results are shown on the left, and relative colony formation efficiencies are on the right. Shown are means of 3 replications; error bars represent SDs. E, Western blot analysis of Annexin A2 in HCT116 cells transfected with a miR-1 precursor molecule or a negative control. Precursor of miR-17, which is abundantly expressed in HCT116 cells and is irrelevant to miR-1, served as another negative control. F, putative miR-1 binding site in the 3′ untranslated region (UTR) of *ANXA2*. A fragment that included the binding site was PCR amplified and cloned into pMIR-REPORT vector. G, reporter assay results using the luciferase vector with the 3′ UTR of *ANXA2* or an empty vector in HCT116 cells cotransfected with a miR-1 precursor, a negative control (Cont), or a miR-17 precursor. Shown are the means of 4 replications; error bars represent SDs. H, wound-healing assay using HCT116 cells transfected with a miR-1 precursor or a negative control. The wound was made 24 hours after transfection, and photographs were taken at the indicated time points. I, Matrigel invasion assay using HCT116 cells transfected with a miR-1 precursor, a negative control, or a miR-17 precursor. Invading cells are indicated by arrowheads. Shown on the right are the means of 3 random microscopic fields per membrane; error bars represent the SDs.

polymerase (pol) II binding patterns (23, 24), evolutionally conserved regions (25), EST mapping (26), and computationally predicted promoters (27, 28). Active promoters are reportedly marked by H3K4me3 (29), and recent studies that have applied such histone marks have successfully identified miRNA gene promoters or TSSs (9, 12). In the present study,

Downloaded from cancerres.aacrjournals.org on April 26, 2012
Copyright © 2011 American Association for Cancer Research

Published OnlineFirst July 6, 2011; DOI:10.1158/0008-5472.CAN-11-1076

we carried out high-resolution ChIP-seq analyses in an effort to detect the chromatin signatures of miRNA genes in colorectal cancer.

Although we were able to identify the putative promoters of a number of miRNAs, the present study has several limitations. First, our strategy to identify miRNA promoters can be applied only to transcriptionally active genes. Second, promoters of 135 miRNAs remain unidentified, although their expression was detected in colorectal cancer cells. The majority of such miRNAs (103 of 135) are located in the intergenic regions, and if we increase our search scope, we may identify putative promoter regions in the further upstream, although the accuracy may be decreased. For example, in DKO cells, we detected abundant expression of placenta-specific miRNAs transcribed from a miRNA cluster on chromosome 19 (C19MC), suggesting these miRNAs are epigenetically silenced in normal adult tissues. We found an H3K4me3 mark around a CGI located approximately 18 kb upstream of the cluster, suggesting that this region may be a putative promoter of C19MC (Supplementary Fig. S13), which is consistent with a recent report that hypermethylation of this CGI is associated with epigenetic silencing of C19MC in human cancer cell lines (30). However, other studies have shown that the Alu repetitive sequences within which C19MC is embedded exhibit RNA pol II or pol III promoter activities (31, 32), but we failed to detect obvious active histone marks in these Alu repeats. These results suggest that C19MC may have multiple promoter regions and point to a limitation of the strategy we employed in the current study.

Despite this limitation, chromatin signatures provided important clues to the identity of epigenetically silenced miRNAs in cancer. In HCT116 cells, for instance, the miR-9-1 promoter showed significant enrichment of active histone marks and mature miR-9 was abundantly expressed (data not shown). On the other hand, lack of H3K4me3 in the same cells and its restoration after DNA demethylation clearly suggest that miR-9-2 and miR-9-3 are epigenetically silenced in these cells, which is indicative of the utility of our strategy. We also noted that chromatin signatures of epileptically silenced miRNA genes exhibit patterns similar to those of protein-coding genes. Recent studies have shown that TSGs with CGI methylation retain repressive histone modifications (H3K9me3 and H3K27me3) even after demethylation (15). A genome-wide analysis of the chromatin signature using ChIP-on-chip in colorectal cancer cells revealed that hypermethylated genes adopt a bivalent chromatin pattern upon DNA demethylation (16). More recently, Jacinto and colleagues found that DNA demethylation never results in restoration of the H3K79me2 mark in TSGs with methylated CGIs, suggesting that such incomplete chromatin reactivation leads to relatively low levels of reexpression (33). In the present study, we found that miRNA genes with methylated CGIs never return to a full euchromatin status after DNA demethylation. In addition, we observed significant overlap between PcG marked miRNAs in ES cells and miRNAs with CGI methylation in cancer cells, suggesting a strong predisposition of these miRNAs toward aberrant DNA methylation in cancer.

Many of the epigenetically silenced miRNA genes we identified have been implicated in human malignancies. miR-124 family, miR-9 family, miR-34b/c, and miR-129-2 were identified by screening for epigenetically silenced miRNAs in colorectal cancer cell lines (5, 6, 13), and their methylation was subsequently found in various cancers (8, 34–36). Methylation-associated silencing of miR-137 was first reported in oral cancer (37), and a recent study revealed its frequent methylation in the early stages of colorectal tumorigenesis (38). The high frequency of CGI hypermethylation in these miRNAs in primary colorectal cancer is suggestive of their tumor suppressor function. It was also recently shown that the muscle-specific miRNAs miR-1 and miR-133a are downregulated in primary colorectal cancer tumors as compared with normal colonic tissues (39). Reduced expression of miR-1 is also found in lung cancer (40), and CGI methylation–mediated silencing of miR-1-1 has been reported in hepatocellular carcinoma (41). In addition, levels of miR-1 expression were diminished in the serum of non–small-cell lung cancer (NSCLC) patients who survived for only a short period, suggesting that it is predictive of prognosis in NSCLC patients (42). Ectopic expression of miR-1 in lung cancer, liver cancer, and rhabdomyosarcoma cells reportedly inhibits cellular growth through suppression of its target genes, which include *MET*, *FOXP1*, and *HDAC4* (40, 41, 43). In the present study, we found frequent methylation of the miR-1-1 promoter CGI in both colorectal adenoma and primary colorectal cancer tissues, suggesting that aberrant methylation of miR-1-1 is an early event in colorectal tumorigenesis. The strong tumor specificity of the methylation indicates that it could be a novel tumor marker for early detection of colorectal neoplasia. Because the tumor suppressor potential of miR-1 has not been tested in colorectal cancer, we conducted a number of functional analyses, and our findings indicate that ectopic expression of miR-1 in colorectal cancer cells suppresses cell growth, colony formation, cell motility, and invasion. In addition, our gene expression analysis revealed that miR-1 could induce global changes in gene expression in colorectal cancer cells, especially genes related to the extracellular region, cell membrane, and wound healing. We identified 2 novel miR-1 target genes, *ANXA2* and *BDNF*, which are frequently overexpressed in cancer and are implicated in invasion and metastasis (20–22). These results are suggestive of the tumor suppressor role of miR-1 and its potential therapeutic application in colorectal cancer.

On the other hand, we unexpectedly detected silencing of several miRNAs with known oncogenic properties. For example, miR-155 is a well-characterized oncogenic miRNA that is overexpressed in various human malignancies (44). Although we found miR-155 to be silenced with CGI methylation in HCT116 cells, its methylation was rarely observed in primary tumors, suggesting that epigenetic silencing of miR-155 may not be functionally important in colorectal cancer. Similarly, miR-196a-1 is reportedly overexpressed in several human malignancies, including esophageal adenocarcinoma and glioblastoma (45, 46). Methylation levels of miR-196a-1 in primary colorectal cancer tumors are lower than in normal colonic tissue, which is in agreement with its possible oncogenic properties in colorectal cancer.

Finally, our chromatin signature analysis revealed that a number of miRNAs without promoter CGIs are also potential

Downloaded from cancerres.aacrjournals.org on April 26, 2012
Copyright © 2011 American Association for Cancer Research

Published OnlineFirst July 6, 2011; DOI:10.1158/0008-5472.CAN-11-1076

targets of epigenetic silencing in colorectal cancer. These miRNAs were identified through restoration of both their expression and H3K4me3 marking after DNA demethylation, whereas the signatures of H3K79me2 and H3K27me3 varied among genes. This category may thus include miRNAs induced by secondary effects of DNA demethylation, such as upregulation of transcription factors. It is noteworthy, however, that some functionally important miRNAs showed chromatin signatures that were distinct from CGI-methylated miRNAs. Upon DNA demethylation, miR-142 and miR-146a exhibited more active chromatin states, which were characterized by enrichment of both H3K4me3 and H3K79me2 marks. Earlier studies implicated their tumor suppressor roles in cancers of various origins. For instance, miR-142 was found to be downregulated in murine and human lung cancer and its expression suppressed cancer cell growth (47). Loss of miR-146a was reported in hormone-refractory prostate cancer (48), and expression of miR-146a suppressed NF-κB activity and metastatic potential in breast and pancreatic cancer cells (49, 50). The abundant expression of miRNAs in normal colon and downregulation in multiple colorectal cancer cell lines indicates their tumor-suppressive properties in colorectal cancer (data not shown), though further study is need to define the functions of miRNAs in colorectal tumorigenesis.

With this study, we provide compelling evidence that both CGI-positive and -negative miRNAs are targets of epigenetic silencing in colorectal cancer. Our data suggest that DNA demethylation can alter the chromatin signatures of numerous miRNAs in cancer and that reexpression of these miRNAs has important relevance to the effects of epigenetic cancer therapy.

Disclosure of Potential Conflicts of Interest

No potential conflicts of interest were disclosed.

Acknowledgments

The authors thank Dr. William F. Goldman for editing the manuscript and M. Ashida for technical assistance.

Grant Support

This study was supported in part by Grants-in-Aid for Scientific Research on Priority Areas (M. Toyota and K. Imai), a Grant-in-Aid for the Third-term Comprehensive 10-year Strategy for Cancer Control (M. Toyota), a Grant-in-Aid for Cancer Research from the Ministry of Health, Labor, and Welfare, Japan (M. Toyota), the A3 foresight program from the Japan Society for Promotion of Science (H. Suzuki), and Grants-in-Aid for Scientific Research (A) from the Japan Society for Promotion of Science (K. Imai).

The costs of publication of this article were defrayed in part by the payment of page charges. This article must therefore be hereby marked *advertisement* in accordance with 18 U.S.C. Section 1734 solely to indicate this fact.

Received March 27, 2011; revised June 28, 2011; accepted June 30, 2011; published OnlineFirst July 6, 2011.

References

1. He L, Hannon GJ. MicroRNAs: small RNAs with a big role in gene regulation. Nat Rev Genet 2004;5:522–31.
2. Esquela-Kerscher A, Slack FJ. Oncomirs—microRNAs with a role in cancer. Nat Rev Cancer 2006;6:259–69.
3. Melo SA, Ropero S, Moutinho C, Aaltonen LA, Yamamoto H, Calin GA, et al. A TARBP2 mutation in human cancer impairs microRNA processing and DICER1 function. Nat Genet 2009;41:365–70.
4. Melo SA, Moutinho C, Ropero S, Calin GA, Rossi S, Spizzo R, et al. A genetic defect in exportin-5 traps precursor microRNAs in the nucleus of cancer cells. Cancer Cell 2010;18:303–15.
5. Lujambio A, Ropero S, Ballestar E, Fraga MF, Cerrato C, Setien F, et al. Genetic unmasking of an epigenetically silenced microRNA in human cancer cells. Cancer Res 2007;67:1424–9.
6. Toyota M, Suzuki H, Sasaki Y, Maruyama R, Imai K, Shinomura Y, et al. Epigenetic silencing of microRNA-34b/c and B-cell translocation gene 4 is associated with CpG island methylation in colorectal cancer. Cancer Res 2008;68:4123–32.
7. Saito Y, Liang G, Egger G, Friedman JM, Chuang JC, Coetzee GA, et al. Specific activation of microRNA-127 with downregulation of the proto-oncogene BCL6 by chromatin-modifying drugs in human cancer cells. Cancer Cell 2006;9:435–43.
8. Suzuki H, Yamamoto E, Nojima M, Kai M, Yamano HO, Yoshikawa K, et al. Methylation-associated silencing of microRNA-34b/c in gastric cancer and its involvement in an epigenetic field defect. Carcinogenesis 2010;31:2066–73.
9. Marson A, Levine SS, Cole MF, Frampton GM, Brambrink T, Johnstone S, et al. Connecting microRNA genes to the core transcriptional regulatory circuitry of embryonic stem cells. Cell 2008;134:521–33.
10. Akino K, Toyota M, Suzuki H, Mita H, Sasaki Y, Ohe-Toyota M, et al. The Ras effector RASSF2 is a novel tumor-suppressor gene in human colorectal cancer. Gastroenterology 2005;129:156–69.
11. Zhang Y, Liu T, Meyer CA, Eeckhoute J, Johnson DS, Bernstein BE, et al. Model-based analysis of ChIP-Seq (MACS). Genome Biol 2008;9:R137.
12. Ozsolak F, Poling LL, Wang Z, Liu H, Liu XS, Roeder RG, et al. Chromatin structure analyses identify miRNA promoters. Genes Dev 2008;22:3172–83.
13. Bandres E, Agirre X, Bitarte N, Ramirez N, Zarate R, Roman-Gomez J, et al. Epigenetic regulation of microRNA expression in colorectal cancer. Int J Cancer 2009;125:2737–43.
14. Kondo Y, Shen L, Cheng AS, Ahmed S, Boumber Y, Charo C, et al. Gene silencing in cancer by histone H3 lysine 27 trimethylation independent of promoter DNA methylation. Nat Genet 2008;40:741–50.
15. McGarvey KM, Fahmer JA, Greene E, Martens J, Jenuwein T, Baylin SB. Silenced tumor suppressor genes reactivated by DNA demethylation do not return to a fully euchromatic chromatin state. Cancer Res 2006;66:3541–9.
16. McGarvey KM, Van Neste L, Cope L, Ohm JE, Herman JG, Van Criekinge W, et al. Defining a chromatin pattern that characterizes DNA-hypermethylated genes in colon cancer cells. Cancer Res 2008;68:5753–9.
17. Rodriguez A, Griffiths-Jones S, Ashurst JL, Bradley A. Identification of mammalian microRNA host genes and transcription units. Genome Res 2004;14:1902–10.
18. Ohm JE, McGarvey KM, Yu X, Cheng L, Schuebel KE, Cope L, et al. A stem cell-like chromatin pattern may predispose tumor suppressor genes to DNA hypermethylation and heritable silencing. Nat Genet 2007;39:237–42.
19. Widschwendter M, Fiegl H, Egle D, Mueller-Holzner E, Spizzo G, Marth C, et al. Epigenetic stem cell signature in cancer. Nat Genet 2007;39:157–8.
20. Emoto K, Yamada Y, Sawada H, Fujimoto H, Ueno M, Takayama T, et al. Annexin II overexpression correlates with stromal tenascin-C overexpression: a prognostic marker in colorectal carcinoma. Cancer 2001;92:1419–26.
21. Diaz VM, Hurtado M, Thomson TM, Reventos J, Paciucci R. Specific interaction of tissue-type plasminogen activator (t-PA) with Annexin II on the membrane of pancreatic cancer cells activates plasminogen and promotes invasion *in vitro*. Gut 2004;53:993–1000.

Downloaded from cancerres.aacrjournals.org on April 26, 2012
Copyright © 2011 American Association for Cancer Research

Published OnlineFirst July 6, 2011; DOI:10.1158/0008-5472.CAN-11-1076

22. Douma S, Van Laar T, Zevenhoven J, Meuwissen R, Van Garderen E, Peeper DS. Suppression of anoikis and induction of metastasis by the neurotrophic receptor TrkB. Nature 2004;430:1034–9.
23. Wang G, Wang Y, Shen C, Huang YW, Huang K, Huang TH, et al. RNA polymerase II binding patterns reveal genomic regions involved in microRNA gene regulation. PLoS One 2010;5:e13798.
24. Corcoran DL, Pandit KV, Gordon B, Bhattacharjee A, Kaminski N, Benos PV. Features of mammalian microRNA promoters emerge from polymerase II chromatin immunoprecipitation data. PLoS One 2009;4:e5279.
25. Fujita S, Iba H. Putative promoter regions of miRNA genes involved in evolutionarily conserved regulatory systems among vertebrates. Bioinformatics 2008;24:303–8.
26. Gu J, He T, Pei Y, Li F, Wang X, Zhang J, et al. Primary transcripts and expressions of mammal intergenic microRNAs detected by mapping ESTs to their flanking sequences. Mamm Genome 2006;17:1033–41.
27. Zhou X, Ruan J, Wang G, Zhang W. Characterization and identification of microRNA core promoters in four model species. PLoS Comput Biol 2007;3:e37.
28. Long YS, Deng GF, Sun XS, Yi YH, Su T, Zhao QH, et al. Identification of the transcriptional promoters in the proximal regions of human microRNA genes. Mol Biol Rep 2010.
29. Mikkelsen TS, Ku M, Jaffe DB, Issac B, Lieberman E, Giannoukos G, et al. Genome-wide maps of chromatin state in pluripotent and lineage-committed cells. Nature 2007;448:553–60.
30. Tsai KW, Kao HW, Chen HC, Chen SJ, Lin WC. Epigenetic control of the expression of a primate-specific microRNA cluster in human cancer cells. Epigenetics 2009;4:587–92.
31. Saito Y, Suzuki H, Tsugawa H, Nakagawa I, Matsuzaki J, Kanai Y, et al. Chromatin remodeling at Alu repeats by epigenetic treatment activates silenced microRNA-512-5p with downregulation of Mcl-1 in human gastric cancer cells. Oncogene 2009;28:2738–44.
32. Borchert GM, Lanier W, Davidson BL. RNA polymerase III transcribes human microRNAs. Nat Struct Mol Biol 2006;13:1097–101.
33. Jacinto FV, Ballestar E, Esteller M. Impaired recruitment of the histone methyltransferase DOT1L contributes to the incomplete reactivation of tumor suppressor genes upon DNA demethylation. Oncogene 2009;28:4212–24.
34. Ando T, Yoshida T, Enomoto S, Asada K, Tatematsu M, Ichinose M, et al. DNA methylation of microRNA genes in gastric mucosae of gastric cancer patients: its possible involvement in the formation of epigenetic field defect. Int J Cancer 2009;124:2367–74.
35. Agirre X, Vilas-Zornoza A, Jimenez-Velasco A, Martin-Subero JI, Cordeu L, Garate L, et al. Epigenetic silencing of the tumor suppressor microRNA Hsa-miR-124a regulates CDK6 expression and confers a poor prognosis in acute lymphoblastic leukemia. Cancer Res 2009;69:4443–53.
36. Huang YW, Liu JC, Deatherage DE, Luo J, Mutch DG, Goodfellow PJ, et al. Epigenetic repression of microRNA-129-2 leads to overexpression of SOX4 oncogene in endometrial cancer. Cancer Res 2009;69:9038–46.
37. Kozaki K, Imoto I, Mogi S, Omura K, Inazawa J. Exploration of tumor-suppressive microRNAs silenced by DNA hypermethylation in oral cancer. Cancer Res 2008;68:2094–105.
38. Balaguer F, Link A, Lozano JJ, Cuatrecasas M, Nagasaka T, Boland CR, et al. Epigenetic silencing of miR-137 is an early event in colorectal carcinogenesis. Cancer Res 2010;70:6609–18.
39. Sarver AL, French AJ, Borralho PM, Thayanithy V, Oberg AL, Silverstein KA, et al. Human colon cancer profiles show differential microRNA expression depending on mismatch repair status and are characteristic of undifferentiated proliferative states. BMC Cancer 2009;9:401.
40. Nasser MW, Datta J, Nuovo G, Kutay H, Motiwala T, Majumder S, et al. Down-regulation of micro-RNA-1 (miR-1) in lung cancer. Suppression of tumorigenic property of lung cancer cells and their sensitization to doxorubicin-induced apoptosis by miR-1. J Biol Chem 2008;283:33394–405.
41. Datta J, Kutay H, Nasser MW, Nuovo GJ, Wang B, Majumder S, et al. Methylation mediated silencing of MicroRNA-1 gene and its role in hepatocellular carcinogenesis. Cancer Res 2008;68:5049–58.
42. Hu Z, Chen X, Zhao Y, Tian T, Jin G, Shu Y, et al. Serum microRNA signatures identified in a genome-wide serum microRNA expression profiling predict survival of non-small-cell lung cancer. J Clin Oncol 2010;28:1721–6.
43. Yan D, Dong Xda E, Chen X, Wang L, Lu C, Wang J, et al. MicroRNA-1/206 targets c-Met and inhibits rhabdomyosarcoma development. J Biol Chem 2009;284:29596–604.
44. Croce CM. Causes and consequences of microRNA dysregulation in cancer. Nat Rev Genet 2009;10:704–14.
45. Maru DM, Singh RR, Hannah C, Albarracin CT, Li YX, Abraham R, et al. MicroRNA-196a is a potential marker of progression during Barrett's metaplasia-dysplasia-invasive adenocarcinoma sequence in esophagus. Am J Pathol 2009;174:1940–8.
46. Guan Y, Mizoguchi M, Yoshimoto K, Hata N, Shono T, Suzuki SO, et al. MiRNA-196 is upregulated in glioblastoma but not in anaplastic astrocytoma and has prognostic significance. Clin Cancer Res 2010;16:4289–97.
47. Liu X, Sempere LF, Galimberti F, Freemantle SJ, Black C, Dragnev KH, et al. Uncovering growth-suppressive MicroRNAs in lung cancer. Clin Cancer Res 2009;15:1177–83.
48. Lin SL, Chiang A, Chang D, Ying SY. Loss of mir-146a function in hormone-refractory prostate cancer. RNA 2008;14:417–24.
49. Bhaumik D, Scott GK, Schokrpur S, Patil CK, Campisi J, Benz CC. Expression of microRNA-146 suppresses NF-kappaB activity with reduction of metastatic potential in breast cancer cells. Oncogene 2008;27:5643–7.
50. Li Y, Vandenboom TG 2nd, Wang Z, Kong D, Ali S, Philip PA, et al. miR-146a suppresses invasion of pancreatic cancer cells. Cancer Res 2010;70:1486–95.

Downloaded from cancerres.aacrjournals.org on April 26, 2012
Copyright © 2011 American Association for Cancer Research

see related editorial on page 470

A Novel Pit Pattern Identifies the Precursor of Colorectal Cancer Derived From Sessile Serrated Adenoma

Tomoaki Kimura, MD[1,7], Eiichiro Yamamoto, MD, PhD[2,3,7], Hiro-o Yamano, MD[1], Hiromu Suzuki, MD, PhD[2,3], Seiko Kamimae, MD[2], Masanori Nojima, MD, PhD, MPH[4], Takeshi Sawada, MD, PhD[2], Masami Ashida, MS[2], Kenjiro Yoshikawa, MD[1], Ryo Takagi, MD, PhD[1], Ryusuke Kato, MD[1], Taku Harada, MD[1], Ryo Suzuki, MD[1,3], Reo Maruyama, MD, PhD[2,3], Masahiro Kai, PhD[2], Kohzoh Imai, MD, PhD[5], Yasuhisa Shinomura, MD, PhD[3], Tamotsu Sugai, MD, PhD[6] and Minoru Toyota, MD, PhD[2]

OBJECTIVES: **Sessile serrated adenomas (SSAs) are known to be precursors of sporadic colorectal cancers (CRCs) with microsatellite instability (MSI), and to be tightly associated with *BRAF* mutation and the CpG island methylator phenotype (CIMP). Consequently, colonoscopic identification of SSAs has important implications for preventing CRCs, but accurate endoscopic diagnosis is often difficult. Our aim was to clarify which endoscopic findings are specific to SSAs.**

METHODS: **The morphological, histological and molecular features of 261 specimens from 226 colorectal tumors were analyzed. Surface microstructures were analyzed using magnifying endoscopy. Mutation in *BRAF* and *KRAS* was examined by pyrosequencing. Methylation of *p16*, *IGFBP7*, *MLH1* and *MINT1*, *-2*, *-12* and *-31* was analyzed using bisulfite pyrosequencing.**

RESULTS: **Through retrospective analysis of a training set ($n=145$), we identified a novel surface microstructure, the Type II open-shape pit pattern (Type II-O), which was specific to SSAs with *BRAF* mutation and CIMP. Subsequent prospective analysis of an independent validation set ($n=116$) confirmed that the Type II-O pattern is highly predictive of SSAs (sensitivity, 65.5%; specificity, 97.3%). *BRAF* mutation and CIMP occurred with significant frequency in Type II-O-positive serrated lesions. Progression of SSAs to more advanced lesions was associated with further accumulation of aberrant DNA methylation and additional morphological changes, including the Type III, IV and V pit patterns.**

CONCLUSIONS: **Our results suggest the Type II-O pit pattern is a useful hallmark of the premalignant stage of CRCs with MSI and CIMP, which could serve to improve the efficacy of colonoscopic surveillance.**

SUPPLEMENTARY MATERIAL is linked to the online version of the paper at http://www.nature.com/ajg

Am J Gastroenterol 2012; 107:460–469; doi:10.1038/ajg.2011.457; published online 10 January 2012

INTRODUCTION

Colorectal cancers (CRCs) arise through the accumulation of multiple genetic changes to oncogenes and tumor suppressor genes, a process often referred to as the adenoma–carcinoma sequence (1). In addition to genetic changes, epigenetic alterations such as DNA methylation also have important roles in silencing cancer-related genes, and a subset of CRCs show hypermethylation of the promoter CpG islands of multiple genes (2,3). This has been termed the CpG island methylator phenotype (CIMP) (3). CRCs with CIMP have several characteristic features, including frequent *BRAF* mutation, *MLH1* methylation, microsatellite instability (MSI) and infrequent *p53* mutation (4–6).

Serrated lesions were initially described by Longacre and Fenoglio-Preiser (7) and include hyperplastic polyps (HPs), sessile serrated adenomas (SSAs) and traditional serrated adenomas (TSAs). The criteria used to categorize serrated lesions as HPs, TSAs or SSAs were defined by Torlakovic *et al.* (8) and Snover *et al.* (9), but distinction between SSAs and HPs is often difficult because of their morphological similarity (10–12). In the past, SSAs were classified as HPs, which were considered to have no malignant potential. However, recent studies have shown that SSAs are mainly observed in the proximal colon and are associated with frequent *BRAF* mutation and CIMP, which suggests SSAs are precursors of CRCs with MSI. By contrast, TSAs are

[1]Department of Gastroenterology, Akita Red Cross Hospital, Akita, Japan; [2]Department of Molecular Biology, Sapporo Medical University, Sapporo, Japan; [3]First Department of Internal Medicine, Sapporo Medical University, Sapporo, Japan; [4]Department of Public Health, Sapporo Medical University, Sapporo, Japan; [5]Division of Novel Therapy for Cancer, The Advanced Clinical Research Center, The Institute of Medical Science, The University of Tokyo, Tokyo, Japan; [6]Department of Pathology, Iwate Medical University, Morioka, Japan; [7]These authors contributed equally to this work. **Correspondence:** Hiromu Suzuki, MD, PhD, Department of Molecular Biology, Sapporo Medical University, S1, W17, Chuo-ku, Sapporo 060-8556, Japan. E-mail: hsuzuki@sapmed.ac.jp
Received 21 June 2011; accepted 15 September 2011

often found in the distal colon and show frequent *KRAS* mutation (13–16).

Colonoscopic identification of serrated lesions and conventional adenomas has important implications for preventing CRCs. However, accurate diagnosis of serrated lesions is often difficult, and it is particularly difficult to distinguish SSAs from HPs solely through colonoscopic observation (12,17). In that regard, high-resolution magnifying colonoscopy is now recognized to be a powerful diagnostic tool for predicting the malignancy of conventional adenomas, the efficacy of which has been confirmed in a number of independent studies (18–21). According to Kudo's classification (18,20), the pit patterns of non-neoplastic lesions are classified as Type I (normal colon) or II (HP), whereas the pit patterns of neoplastic lesions are classified as Types III, IV and V. Because Type II pits are indicative of non-neoplastic HP lesions and are also observed in serrated lesions, SSAs and TSAs were considered to be benign when the pit pattern classification was established (17,22,23). But given the aforementioned evidence that SSAs may be precursors of CRCs with MSI, it would seem necessary to refine the criteria for the Type II pit pattern, based on its histological and molecular characteristics.

In the present study, we hypothesized that SSAs exhibit morphological features that are distinct from the features of non-neoplastic lesions or conventional adenomas. To test that idea, we carried out an integrative analysis of the morphological, histological and molecular features of serrated lesions with the ultimate aim of establishing more accurate diagnostic criteria.

METHODS

Patients and tissue specimens

All specimens of colorectal serrated lesions were collected from Japanese patients who underwent endoscopic mucosal resection of a colorectal tumor at Akita Red Cross Hospital. The training set included 145 specimens from 122 serrated lesions or conventional adenomas collected between January 2009 and December 2009. An independent validation set included 116 specimens from 104 serrated lesions or conventional adenomas, which were prospectively collected between January 2010 and December 2010. Informed consent was obtained from all patients before collection of the specimens. Approval of this study was obtained from the Institutional Review Board of Akita Red Cross Hospital and Sapporo Medical University. Genomic DNA was extracted from biopsy specimens using the standard phenol-chloroform procedure.

Endoscopic analysis

High-resolution magnifying endoscopes (CF260AZI; Olympus, Tokyo, Japan) were used for all colonoscopic analyses. Participating in this study were 10 endoscopists, all of whom were trained as gastroenterologists for at least 3 years. Among them, moreover, four had experience with more than 1,000 cases before this study. All serrated lesions detected by colonoscopy were observed at high magnification, using indigo carmine dye. Surface microstructures were classified according to the Kudo's pit pattern classification system (18,20). Biopsy specimens were obtained from all of the lesions for genomic DNA extraction, after which the lesions were treated by endoscopic mucosal resection or endoscopic submucosal dissection. In principle, one biopsy specimen was obtained from each lesion. If more than two pit patterns were observed in a single lesion, a biopsy specimen was obtained from each pit pattern portion.

Histological analysis

Histological findings for all specimens were evaluated by a gastrointestinal pathologist (TS) who was blinded to the clinical and molecular information. Conventional adenoma was diagnosed using the standard criteria. Conventional adenoma with serration (Ad + se) was included with the serrated lesions (15). Serrated lesions (HPs, SSAs and TSAs) were classified on the basis of the criteria previously described by Torlakovic *et al.* (8). In this study, serrated lesions that did not satisfy the criteria for SSA or TSA were defined as intermediate (IM) and classified in the same category as HP (HP/IM). Mixed serrated lesions composed of HP/IM, SSA, TSA, adenomatous change (Ad-C) or high-grade dysplasia (HGD) were evaluated on the basis of each component and described as HP/IM + Ad-C, SSA + Ad-C or SSA + HGD.

DNA methylation analysis

CpG island methylation was analyzed as described previously (24). Briefly, genomic DNA (1 μg) was modified with sodium bisulfite using an EpiTect Bisulfite Kit (QIAGEN, Hilden, Germany). Pyrosequencing was carried out using a PSQ96 system with a PyroGold reagent Kit (QIAGEN), and the results were analyzed using Q-CpG software (QIAGEN). A cutoff value of 15% was used to define genes as methylation-positive. Tumors were defined as CIMP-positive when methylation was detected in three or more loci of the five markers (*MINT1*, *MINT2*, *MINT12*, *MINT31* and *p16*). Sequence information for primers and probes are summarized in **Supplementary Table 1**.

Mutation analysis

Mutation of codon 600 of *BRAF* and codons 12 and 13 of *KRAS* was examined by pyrosequencing using *BRAF* and *KRAS* pyro kits (QIAGEN) according to the manufacturer's instructions.

Analysis of MSI

MSI was assessed as described previously (25). The primers proposed by the National Cancer Institute Workshop on Microsatellite Instability (BAT25, BAT26, D5S346, D2S123, D17S250) were used (26). MSI was defined by the presence of abnormally sized bands in the tumor sample, as compared with a sample of the corresponding normal DNA. A tumor sample was defined as MSI-positive when two or more markers showed instability.

Statistical analysis

To compare differences in continuous variables between groups, a *t*-test or ANOVA with *post-hoc* Tukey test was performed. Fisher's exact test or χ^2-test was used for analysis of categorical data. Odds ratios were calculated using logistic regression models. Values of $P < 0.05$ (two-sided) were considered significant. Receiver operating characteristic curves for diagnosis of colorectal

© 2012 by the American College of Gastroenterology

tumors with *BRAF* mutations and CIMP were constructed, based on the probability in each leaf of the decision tree. All statistical analyses were carried out using SPSS statistics 18 (IBM Corporation, Somers, NY).

RESULTS

Type II open-pit pattern is a specific feature of SSAs

To achieve a more accurate colonoscopic diagnosis of SSAs, we first examined the pit patterns in a series of histologically defined serrated lesions ($n=69$) and conventional adenomatous lesions ($n=76$) as a training set (**Supplementary Figure 1**). Through this retrospective study, we identified an interesting pit pattern that was specific to SSAs (**Figure 1**). We termed this pattern Type II-open (Type II-O), because it was similar to the conventional Type II pattern, but the pits were wider and more rounded in shape, reflecting dilatation of the crypts. The shapes of the Type II-O pits also differed from those of Type I pits, in that they were larger in size with serrations surrounding the pit. Lesions with Type II-O pits often showed conventional Type II pits in the surrounding fields.

We categorized the lesions into two groups, depending upon the presence of Type II-O pits, and then examined the relationship between the Type II-O pit pattern and several molecular alterations (**Table 1**). Importantly, none of the conventional adenomas exhibited the Type II-O pit pattern, and among the serrated lesions, the Type II-O pit pattern was specific to SSAs. A majority of Type II-O pit-positive lesions exhibited *BRAF* mutations, whereas *KRAS* mutations were more prevalent among Type II-O-negative lesions (**Table 1**). Because *BRAF* mutation is strongly associated with CIMP in CRCs, we determined the CIMP status of the lesions by assessing the methylation of five CIMP markers (*MINT1*, *-2*, *-12*, *-31* and *p16*). As expected, a majority of the lesions with Type II-O pits was CIMP-positive, and showed elevated levels of *p16* methylation (**Table 1**, **Figure 2**). Type II-O-positive lesions also showed elevated methylation of *IGFBP7*, another CIMP-associated gene (**Figure 2**) (27).

To confirm our findings, we carried out a prospective study using an independent validation set, which included serrated lesions ($n=55$) and conventional adenomas ($n=61$; **Supplementary Figure 1**). With this validation set, we initially made a colonoscopic diagnosis of each lesion, and then examined its histological and molecular features. Again, we observed that Type II-O pits were specific to SSAs with *BRAF* mutations and CIMP (**Table 1**). As shown in **Figure 2**, lesions with Type II-O pits exhibited elevated levels of *p16* and *IGFBP7* methylation. These results strongly suggest that morphological observations made using magnifying colonoscopy can effectively identify one of the earliest steps in the CIMP and MSI pathway.

Clinicopathological features of Type II-O-positive lesions

The clinicopathological characteristics of the patients are summarized in **Table 2**. There were no statistically significant differences

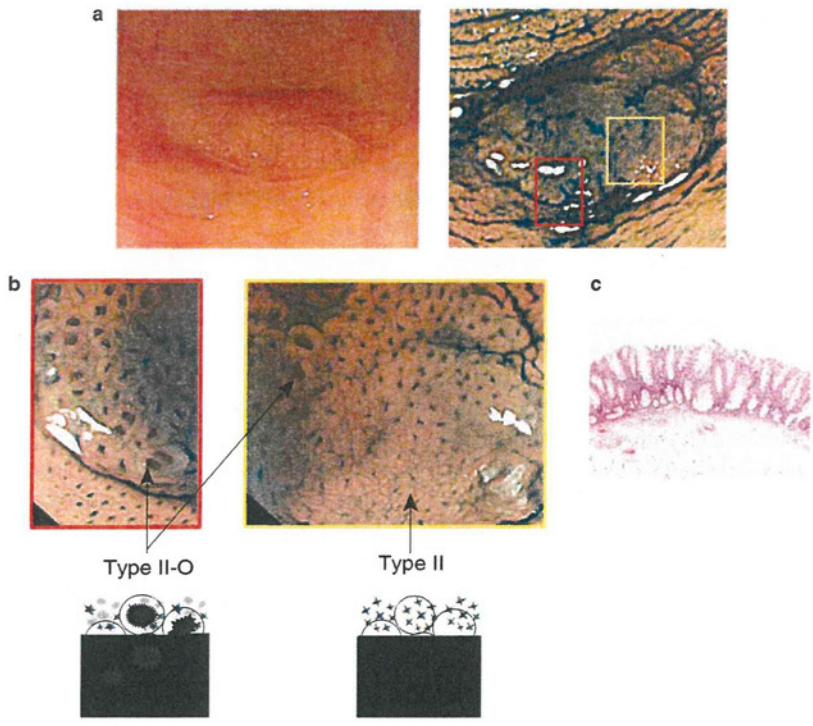

Figure 1. Identification of the Type II open-shape (Type II-O) pit pattern in sessile serrated adenomas (SSAs). (**a**) Colonoscopic view of a representative SSA with (right) and without indigo carmine dye (left). (**b**) Magnified views of the SSA areas indicated by the red and yellow boxes in panel **a**. Left panel: the majority of the pits are Type II-O. Right panel: the upper region is covered by Type II-O pits, whereas the lower region is covered by conventional Type II pits. Schematic diagrams of Type II and Type II-O pits are shown below. (**c**) Histological appearance of the SSA with Type II-O pits.

Table 1. Association of the Type II-O pattern with histological and molecular features

	SSA		*KRAS*		*BRAF*		CIMP	
	Yes	No	Mut	WT	Mut	WT	Positive	Negative
(a) Training Set								
Serrated lesions								
Type II-O								
Positive	15	0	1	14	14	1	11	4
Negative	0	31	9	22	9	22	3	28
Conventional adenoma								
Type II-O								
Positive	0	0	0	0	0	0	0	0
Negative	0	76	25	51	1	75	2	74
Sensitivity	1.000		0.029		0.583		0.688	
Specificity	1.000		0.839		0.99		0.962	
(b) Validation Set								
Serrated lesions								
Type II-O								
Positive	19	2	1	20	18	3	15	6
Negative	10	12	4	18	10	12	5	17
Conventional adenoma								
Type II-O								
Positive	0	0	0	0	0	0	0	0
Negative	0	61	16	45	1	60	1	60
Sensitivity	0.655		0.001		0.621		0.714	
Specificity	0.973		0.759		0.960		0.928	
OR (95% CI)	69.4 (14–343.5)		0.2 (0.0–1.2)		39.3 (9.9–155.7)		32.1 (9.1–113.1)	

CI, confidence interval; CIMP, CpG island methylator phenotype; Mut, mutant; OR, odds ratio; SSA, sessile serrated adenoma; Type II-O, Type II open-shape; WT, wild type.

with respect to age, lesion morphology and size between patients with Type II-O pit-positive and -negative lesions. In addition, the majority of lesions with Type II-O pits were located on the right side of the colon, which is consistent with the well-defined characteristics of CIMP-positive CRCs. Histologically, a large majority of Type II-O pit-positive lesions were diagnosed as SSA. A subset of lesions exhibited more advanced pit patterns in addition to the Type II-O pits (Type II-O plus Type III, IV or V), and those specimens showed mixtures of SSA and Ad-C, TSA or HGD (**Table 2**). By contrast, a majority of the conventional Type II lesions showed HP/IM histology, and a subset of Type II lesions that contained additional Type IV patterns showed a mixture of HP/IM and Ad-C or TSA (**Table 2**).

Molecular signatures define the progression of Type II-O-positive serrated lesions

Our observations summarized above suggest that serrated lesions with Type II-O pits differ from those with conventional Type II pits, and that they represent a premalignant stage of CIMP-positive CRCs. To confirm this hypothesis, we next examined in detail the molecular features of mixed serrated lesions in which Type II or II-O pits were present along with more advanced pits (Type III, IV or V; **Figure 3a-d**, **Supplementary Figure 2**). In lesions with Type II-O plus Type IV or V pits, both the Type II-O subcomponents and the Type IV or V subcomponents exhibited similar molecular features (e.g., *BRAF* mutation and CIMP), though they differed histologically (i.e., SSAs in the Type II-O components vs. TSAs, Ad-Cs or HGDs in the Type IV or V components; **Figure 3e**, **Supplementary Table 2**). In addition, levels of *p16* and *MLH1* methylation were higher in lesions with Type II-O pits plus more advanced pits than in lesions with only Type II-O pits (**Supplementary Figure 3**). MSI was observed only in portions with a Type V pit pattern (**Supplementary Figure 2**, **Supplementary Table 2**). These molecular signatures strongly suggest that Type IV and V subcomponents develop from coexisting SSAs.

In contrast to lesions with Type II-O pits, those without Type II-O pits showed much lower frequencies of *BRAF* mutation and CIMP, but higher frequencies of *KRAS* mutations (**Figure 3e**, **Supplementary Table 2**). And although Type II-O pit-negative lesions with advanced pit patterns (e.g., Type II plus Type IV lesions) did

© 2012 by the American College of Gastroenterology

COLON/SMALL BOWEL